Multiuser Two-Way Relaying Schemes for UWB Communication

Zahra Ahmadian, Lutz Lampe and Jan Mietzner
Department of Electrical and Computer Engineering
University of British Columbia, Canada
Email: {zahraa, Lampe}@ece.ubc.ca, jan.mietzner@ieee.org

***Abstract*—In this paper we propose multiuser two-way relaying strategies for pairwise internode communication in a network consisting of ultra-wideband (UWB) transceivers with limited signal processing capability, via a central relay unit. We propose reducing the complexity associated with the design of filters at the relay by using pre/post-rake processing in conjunction with optimized filtering at the relay. Two relaying strategies relevant to multipath fading channels, namely detect-and-forward and filter-and-forward with self-interference cancelation, are considered. For both methods, we start with a convex optimization problem formulation with closed-form solutions, then extend the design to the more general case which is a non-convex problem and use an alternating optimization algorithm to solve the design problems. Furthermore, for both design schemes widely linear design formulations are devised. The presented numerical results demonstrate the capability of the proposed design schemes in establishing a reliable communication link between nodes with limited signal processing power and in absence of a direct link.**

***Index Terms*—Detect-and-forward relaying, filter-and-forward relaying, intersymbol interference, multi-way relaying, multiuser interference, multiuser two-way relaying, pre-rake filtering, self-interference cancelation, ultra-wideband (UWB), UWB relay communication.**

I. Introduction

There is an ongoing quest for wireless solutions that satisfy criteria such as low power consumption, security and reliability, in a network of low complexity nodes. Examples of applications for such a network setup are wire replacement in personal area networks for multimedia communications [1], intravehicle communication [2] and the more recent wireless interchip communication [3]. One of the potential solutions that can efficiently provide most of these features is an ultra-wideband (UWB) based communication system with a central station and large number of low complexity nodes, where the complexity is shifted from the nodes to the central transceiver unit [4]. In such a system reliable communication between the central unit and the nodes is achieved by use of pre-rake and pre-equalization filters at the central unit. Considering the asymmetric signal processing capability at the nodes and the central unit, it is possible to achieve reliable internode links via relaying through the central unit.

Relaying can play a significant role in extending the range and throughput of UWB systems, where the communication range is typically limited to less than 10 meters due to restrictions on average power spectral density [5]. In particular, multi-way relaying which has higher spectral efficiency compared to one-way and two-way relaying schemes [6], has the potential for enabling high data rate UWB links [7]. Multiuser two-way relaying is a special case of multi-way relaying, where multiple pairwise links are established simultaneously through the relay.

Part of this work has been submitted for presentation at the 2014 IEEE Vehicular Technology Conference (VTC-Fall).

The completion of this research was made possible thanks to funding from the National Sciences and Engineering Research Council of Canada (NSERC).

A. Related Work and Contributions

There exists a large body of literature on relaying and the many variants of relaying protocols. In the following we start by describing some of the relevant work for relaying over frequency-flat channels and then narrow it down to methods tailored for frequency-selective channels and UWB relaying.

Relaying over frequency-flat channels with multiple-input multiple-output (MIMO) precoding at the relay has been studied in [8]–[12]. In reference [8], two-way amplify-and-forward (AF) relaying with transmit and receiver beam-forming at the source and destination and precoding at the central relay for a single pair of nodes is considered. Two design strategies based on zero-forcing and a minimum mean-square error (MMSE) criterion are developed for the relay pre-coding matrix. Multiuser two-way relaying with MIMO precoding at the relay is considered in [9], where an iterative approach for the joint design of the relay pre-coder matrix and the receive beam-forming at the destination for multiple pairs of nodes is derived. The joint design of source and relay precoders for multi-way relaying has been considered in [11], [12]. In [11], the multi-way relaying network operates as a secondary system in the presence of primary user transmission, and in [12], the effect of channel estimation errors in a multi-way relaying system with pre-coding at the source nodes and the relay and mean-square error (MSE) filtering at the destination nodes is studied.

From the above literature review we note that multi-way relaying is performed by implementing a) precoders at the source nodes and the relay, b) precoding at the relay and filtering at the destination nodes, or c) pre-coding at the source nodes and the relay plus destination node filtering/beam-forming. Problem formulations involving the *joint* design of precoders at the relay and pre-coding or receiver-side processing at the source and destination are non-convex, and hence iterative approaches that decouple the overall problems into a number

of convex sub-problems have been suggested. These iterative methods mostly apply alternating optimization (AO) [13], which is a method based on optimizing a function jointly over a number of variables by alternating restricted optimizations over non-overlapping subsets of variables.

The presence of intersymbol interference (ISI) differentiates relaying over frequency-selective channels from that over frequency-flat fading channels. An alternative to AF relaying, for relaying over frequency-selective channels, is the filter-and-forward (FF) method that attempts to partially resolve the ISI prior to forwarding. One-way FF relaying was first introduced in [14]. Reference [15] offers an extension of this work for one-way relaying when a direct link between source and destination exists and equalization is performed at the destination node. Two-way FF relaying with multiple antennas was considered in [16]–[18]. In reference [16], two-way FF relaying was optimized according to a worst-case signal-to-interference and noise ratio (SINR) maximization criterion and an algorithm based on bisection search was proposed to solve the relaxed problem. The design of equalization filters at the destination nodes was also addressed as part of the design. In [17], worst-case SINR maximization as well as transmit power minimization design formulations were proposed. Similar to [16], for the worst-case SINR maximization problem, a one-dimensional search approach was used to solve a relaxed version of the problem. In reference [18], the two-way FF relaying from [17] was extended to the case of multiuser two-way FF relaying using the same worst-case SINR maximization problem formulation.

In the UWB literature, one of the early works that considered half-duplex AF relaying for impulse radio UWB (IR-UWB) with pulse-position modulation is [19]. References [20] and [21] propose one-way UWB relaying for time-hopped UWB transmission schemes. Furthermore, [22], [23] consider two-way relaying for transmit-reference UWB communication. Differential schemes with non-coherent AF for single and multiple-hop one-way relaying are developed in [24] and [25], respectively. One-way relaying with pre/post-rake combining at the relay was considered in [26] for UWB signaling with guard intervals. In [27] one-way decouple and forward relaying with rake receivers at the destination node was considered. All of the mentioned methods cannot handle multi-way relaying links. In fact, to the best of our knowledge, neither multi-way relaying nor its special case multiuser two-way relaying, for UWB communication has been considered in the literature yet.

Motivated by this fact, in this paper multiuser two-way relaying schemes for pairwise internode UWB communication are proposed. In particular, we consider direct-sequence UWB (DS-UWB), which facilitates coping with ISI and multiple-user interference (MUI) and supports high data rate transmission. Different from the available literature on relaying over frequency-selective channels, we propose the combination of post/pre-rake filtering and optimized post/pre-equalization filters at the relay for pairwise internode communication. Furthermore, we consider filter optimization based on a sum-MSE minimization design criterion which allows us to develop convex problem formulations for improving the overall link performance. The combination of the pre-rake and pre-equalization filtering (PEF) has been considered for downlink of a multiuser DS-UWB system in [4], [28], where in [4], two design strategies based on a) minimizing the sum MSE and b) minimizing the transmit power were introduced. In [28], a robust PEF design strategy for minimizing the transmit power while achieving pre-defined MSE levels in the presence of imperfect channel state information was considered.

The first design scheme considered in this paper is based on detect-and-forward (DTF) relaying, and the second one uses FF relaying. Due to the large delay spread of UWB channels, the FF strategy requires filter lengths similar to the length of the overall impulse response between the source node and the destination node. The optimization of such long filters can be computationally demanding. It was shown in [4] that the combination of the pre-rake and pre-equalization filtering can efficiently reduce the optimized filter length. Such a combination can be applied to the design of the central relay in the downlink phase (i.e., transmission from the relay to the destination nodes) to utilize the available channel information at the relay for optimizing the filter coefficients. For both DTF and FF relaying schemes, an alternative design based on a modified MSE formulation [29] is proposed that leads to improved performance. The problem is however non-convex and we present an iterative solver following the AO principle. Finally, we extend our multiuser two-way relaying design strategies to the widely linear (WL) case, which exploits the fact that most DS-UWB systems use real-valued modulation [30]. The presented numerical results demonstrate that the proposed multiuser two-way relaying schemes are well suited to establish reliable communication links over UWB channels between nodes with limited signal processing power.

B. Organization and Notation

The remainder of this paper is organized as follows. In Section II, we develop filter designs for multiuser two-way DTF relaying with DS-UWB. The case of FF relaying is dealt with in Section III. Numerical results demonstrating the advantages of the proposed designs are discussed in Section IV. Section V concludes the paper.

We use the following notations. $\mathcal{E}\{.\}$, $[.]^T$, $[.]^H$, $[.]^*$, $\|.\|$, $\Re\{.\}$, $\Im\{.\}$ and $\mathrm{diag}\{.\}$ denote statistical expectation, transposition, Hermitian transposition, complex conjugation, the Euclidean norm of a vector, the real and imaginary part of a complex number (applied element-wise in the case of vectors or matrices), and a (block) diagonal matrix, respectively. $[.]*[.]$ stands for linear convolution, and small and capital bold fonts denote vectors and matrices, respectively. $\mathbf{0}_n$ is the $n\times 1$ vector of all zeros.

II. Multiuser Two-Way Detect-and-Forward Relaying

In this section the system model and the filter design for multiuser two-way DTF relaying between U nodes via a central relay is described. Pairs of nodes establish a bi-directional communication through the relay, so that we have in total U links being supported by the relay. We use notations

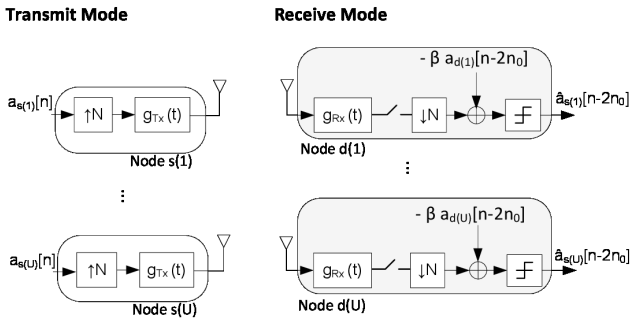

Fig. 1. Block diagram of the source/destination nodes in transmit and receive modes.

$s(u)$ and $d(u)$ to refer to the source and destination node of the u^{th} link, respectively ($u = 1, \ldots, U$).

A. System Model

The block diagram of the source/destination nodes for the considered multiuser two-way relay network is shown in Figure 1. The nodes are single antenna units with limited signal processing capability, while the central relay node, depicted in Figure 2, is equipped with multiple antennas ($M > 1$) and possesses more advanced signal processing capabilities. The network uses a half-duplex two-phase multiple access and broadcast schedule as follows. During the first phase (uplink), all U nodes send their message to the central relay simultaneously. In the second phase (downlink), the relay processes and broadcasts the sum of all node messages through its M antennas.

Source/Destination Transceiver Node: The block diagram representing the node operation in transmit and receive mode is shown in Figure 1. During the uplink phase, the data symbols at the source node of the u^{th} link, $a_{s(u)}[n]$, are upsampled and passed through a pulse shaping filter $g_{\text{Tx}}(t)$ before transmission. The upsampling process is equivalent to having a spreading sequence consisting of a one followed by $N-1$ zeros and it reduces the average transmit power and the ISI. The data symbols, $a_{s(u)}[n]$, are from a binary phase-shift keying (BPSK) constellation with unit average power. In the receive mode, the signal at the node is processed with a noise rejection filter $g_{\text{Rx}}(t)$, downsampled and passed to the detector. Prior to detection it is possible to perform self-interference cancelation by subtracting the destination node's own message from the received signal (the term $-\beta a_{d(u)}[n-2n_0]$ in Figure 1) which will be discussed in the upcoming sections. For the BPSK modulated signal, the detection is performed according to

$$\hat{a}_{s(u)}[n-2n_0] = \text{sign}\Big[\Re\{r_{d(u)}[n]\}\Big] \,, \tag{1}$$

where $r_{d(u)}[n]$ denotes the complex baseband received signal at the slicer input. The delay n_0 is set depending on the processing at the relay and is described in the upcoming sections.

Channel: For the UWB communication channel model, we use the modified Saleh-Valenzuela multipath fading model from [31]. The equivalent baseband discrete time channel between the source node $s(u)$ and the m^{th} antenna at the relay is written as

$$h_{s(u),m}[k] = g_{\text{Tx}}(t) * h_{s(u),m}(t) * g_{\text{Rx}}(t)|_{t=kT/N} \,, \tag{2}$$

where $h_{s(u),m}(t)$ is the continuous-time channel impulse response between the source node $s(u)$ and the m^{th} antenna at the relay, T is the symbol duration, and N is the chip upsampling factor. The discrete-time channel between the m^{th} antenna at the relay and the destination node $d(u)$ is denoted as $h_{d(u),m}[k]$ and has a description similar to (2). For simplicity and practical relevance the filters $g_{\text{Tx}}(t)$ and $g_{\text{Rx}}(t)$ as well as the upsampling factor N are assumed to be identical for all nodes.

Central Relay: The central relay structure in the two phase operation is shown in Figure 2.

The received signal at the relay antennas contains the messages transmitted from all of the source nodes. Considering the signal route for detection of the message from the source user $s(u)$, intended for destination user $d(u)$, the received signal at each of the relay antennas is passed through a rake combining filter $\boldsymbol{p}_{s(u),m}$ of length L_p, a downsampler and a post-equalizing filter $\boldsymbol{f}^{\text{UL}}_{s(u),m}$ of length L_f^{UL}, where $m = 1, \ldots, M$ is the relay antenna index. The detector at the relay then makes a decision on $\hat{a}_{s(u)}[n-n_0]$ based on the sum of the processed signals from all the antennas. Here, n_0 is the delay associated with equalizing, and it is set as $n_0 = \lceil \frac{NL_f+2N+2L_p-k_0-4}{N} \rceil /2$ [4]. Note that the decision delay at the receiving node is $2n_0$ as per Eq. (1). The detected symbol is then processed as per block diagram in Figure 2, for transmission to user $d(u)$. It is passed through pre-equalization filter $\boldsymbol{f}_{d(u),m}$, upsampled and pre-rake combined with pre-rake filter $\boldsymbol{p}_{d(u),m}$. The sum of all outgoing messages is then transmitted via the M relay antennas. The task of the pre-rake filter is to focus the channel energy in a few remaining channel taps (limit ISI) and to provide decorrelation between the signals of multiple users. The task of the PEF is to eliminate residual intersymbol and multiuser interference. In UWB systems, rake processing alone does not offer sufficient interference suppression, due to the large delay spread common for UWB communication channels, therefore equalization or pre-processing is typically applied to limit the interference e.g. [32], [33].

The post/pre-rake combining filters $p_{s(u),m}[k]$ and $p_{d(u),m}[k]$ are set as the time reversed conjugate of the estimated channel impulse response of length L_h, i.e., $p_{s(u),m}[k] = (h_{s(u),m}[L_p - k - 1])^*$ and $p_{d(u),m}[k] = (h_{d(u),m}[L_p - k - 1])^*$. The case $L_p = L_h$ corresponds to all-post/pre-rake combining [34]. The relaying method can be extended to other rake combining techniques (such as partial-post/pre-rake combining with $L_p < L_h$) as well.

Let us consider the signal route for data symbol $a_{s(\ell)}[n]$ ($\ell \neq u$) received via the relay's m^{th} antenna and processed by rake filter $\boldsymbol{p}_{s(u),m}$. The overall impulse response after downsampling can then be defined as $w^{\text{UL}}_{s(\ell),m,s(u)}[k] = h_{s(\ell),m}[k] * p_{s(u),m}[k]$. Using this definition, the received signal at the input of the detector for the message from the source

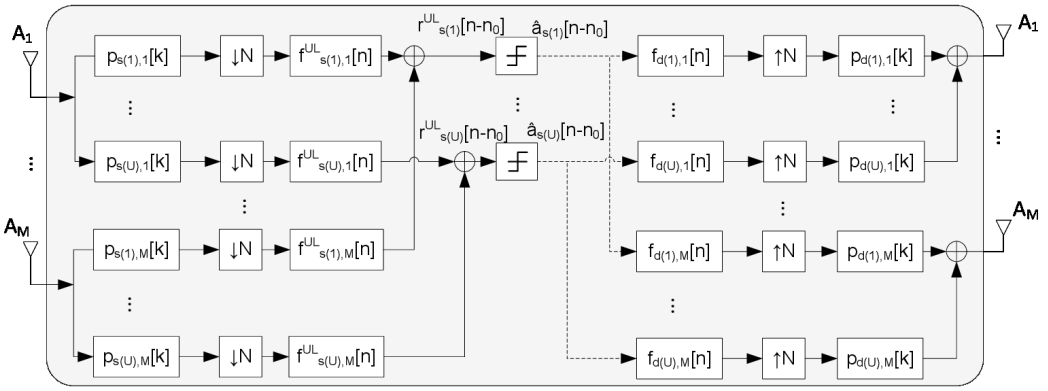

Fig. 2. Block diagram of the central unit for the two phase DTF relaying.

node $s(u)$ can be described as (see Figure 2)

$$r^{\mathrm{UL}}_{s(u)}[n] = \sum_{\ell=1}^{U} (\boldsymbol{f}^{\mathrm{UL}}_{s(u)})^H (\boldsymbol{W}^{\mathrm{UL}}_{s(\ell),s(u)})^H \boldsymbol{a}_{s(\ell)}[n] + z_R[n] \ , \quad (3)$$

where

- $\boldsymbol{f}^{\mathrm{UL}}_{s(u)} = [(\boldsymbol{f}^{\mathrm{UL}}_{s(u),1})^T, \ldots, (\boldsymbol{f}^{\mathrm{UL}}_{s(u),M})^T]^T$ is the vector of M concatenated uplink equalizing filter coefficient vectors $\boldsymbol{f}^{\mathrm{UL}}_{s(u),m} = [f^{\mathrm{UL}}_{s(u),m}[0], \ldots, f^{\mathrm{UL}}_{s(u),m}[L^{\mathrm{UL}}_f - 1]]^H$, for source node $s(u)$,
- $\boldsymbol{W}^{\mathrm{UL}}_{s(\ell),s(u)} = [\boldsymbol{W}^{\mathrm{UL}}_{s(\ell),1,s(u)}, \ldots, \boldsymbol{W}^{\mathrm{UL}}_{s(\ell),M,s(u)}] \in \mathbb{C}^{L_t \times M L^{\mathrm{UL}}_f}$ is a block matrix with Toeplitz block components, $\boldsymbol{W}^{\mathrm{UL}}_{s(\ell),m,s(u)}$,
- $\boldsymbol{W}^{\mathrm{UL}}_{s(\ell),m,s(u)}$ is defined with first row $[(w^{\mathrm{UL}}_{d(\ell),m,d(u)}[k_0])^H, \boldsymbol{0}^T_{L^{\mathrm{UL}}_f - 1}]$, with sampling phase k_0 set as $k_0 = L_p + N - 2 - N\lfloor (L_p + N - 2)/N \rfloor$, and first column vector $[w^{\mathrm{UL}}_{d(\ell),m,d(u)}[k_0], \ldots, w^{\mathrm{UL}}_{d(\ell),m,d(u)}[N(L_w - 1) + k_0], \boldsymbol{0}^T_{L^{\mathrm{UL}}_f - 1}]^H$,
- $L_w = \lceil (L_p + L_h + 2N - 3 - k_0)/N \rceil$ is the length of the overall channel impulse response,
- the vector $\boldsymbol{a}_{s(\ell)}[n] = [a_{s(\ell)}[n], \ldots, a_{s(\ell)}[n - L_t + 1]]^T$ is the $L_t \times 1$ vector of data symbols at the source node $s(\ell)$, and $L_t = L_w + L^{\mathrm{UL}}_f - 1$,
- $z_R[n]$ is the colored noise at the input of the detector.

The variance of $z_R[n]$ can be written in terms of the equalization filter coefficients, as $\sigma^2_{z_R} = \sum_{\ell=1}^{U} (\boldsymbol{f}^{\mathrm{UL}}_{s(\ell)})^H \boldsymbol{P}^H_{s(\ell)} \boldsymbol{P}_{s(\ell)} \boldsymbol{f}^{\mathrm{UL}}_{s(\ell)}$, where $\boldsymbol{P}_{s(\ell)} = \mathrm{diag}\{\boldsymbol{P}_{s(\ell),1}, \ldots, \boldsymbol{P}_{s(\ell),M}\} \in \mathbb{C}^{L_z \times M L_f}$ and $\boldsymbol{P}_{s(\ell),m}$ are Toeplitz matrices with first row $[p_{s(\ell),m}[0], \boldsymbol{0}_{L^{\mathrm{UL}}_f - 1}]$ and first column $[p_{s(\ell),m}[0], \ldots, p_{s(\ell),m}[L_z - L^{\mathrm{UL}}_f + 1], \boldsymbol{0}_{L^{\mathrm{UL}}_f - 1}]^H$, $L_z = L_p + L^{\mathrm{UL}}_f - 1$.

Next we proceed to find the matrix-form signal representation for the downlink phase, which is similar to the downlink received signal representation from [4]. Defining the overall impulse response including pre-rake combining for destination node $d(\ell)$ and the channel impulse response between the relay's m^{th} antenna and destination node $d(u)$ as $w_{d(\ell),m,d(u)}[k] = p_{d(\ell),m}[k] * h_{d(u),m}[k]$, the received signal at the destination node $d(u)$ during the second transmission phase is described as

$$r_{d(u)}[n] = \sum_{\ell=1}^{U} \boldsymbol{f}^H_{d(\ell)} \boldsymbol{W}^H_{d(\ell),d(u)} \hat{\boldsymbol{a}}_{s(\ell)}[n - n_0] + z_{d(u)}[n] \ , \quad (4)$$

where

- $\boldsymbol{f}_{d(u)} = [\boldsymbol{f}^T_{d(u),1}, \ldots, \boldsymbol{f}^T_{d(u),M}]^T$ is the vector containing the M concatenated pre-equalization filter coefficient vectors $\boldsymbol{f}_{d(u),m}$, for destination node $d(u)$,
- $\boldsymbol{f}_{d(u),m} = [f_{d(u),m}[0], \ldots, f_{d(u),m}[L_f - 1]]^H$,
- the matrix $\boldsymbol{W}_{d(\ell),d(u)}$ is the convolution-matrix containing the overall channel impulse response coefficients. It is defined as $\boldsymbol{W}_{d(\ell),d(u)} = [\boldsymbol{W}_{d(\ell),1,d(u)}, \ldots, \boldsymbol{W}_{d(\ell),M,d(u)}] \in \mathbb{C}^{L_t \times M L_f}$ and is a block matrix with Toeplitz block components,
- $\boldsymbol{W}_{d(\ell),m,d(u)} \in \mathbb{C}^{L_t \times L_f}$ is a Toeplitz matrix with first row $[w^H_{d(\ell),m,d(u)}[k_0], \boldsymbol{0}^T_{L_f - 1}]$ and first column vector $[w_{d(\ell),m,d(u)}[k_0], \ldots, w_{d(\ell),m,d(u)}[N(L_w - 1) + k_0], \boldsymbol{0}^T_{L_f - 1}]^H$, where $L_w = \lceil (L_p + L_h + 2N - 3 - k_0)/N \rceil$ is the length of the overall channel impulse response and $L_t = L_w + L_f - 1$,
- $\hat{\boldsymbol{a}}_{s(\ell)}[n - n_0] = [\hat{a}_{s(\ell)}[n - n_0], \ldots, \hat{a}_{s(\ell)}[n - n_0 - L_t + 1]]^T$ is the $L_t \times 1$ vector of estimated data symbols of the source node $s(\ell)$,
- $z_{d(u)}[n]$ is the white Gaussian noise at the destination node with variance $\sigma^2_{d(u)}$.

The average transmit power for the second transmit phase at the relay is written as

$$P = \sum_{u=1}^{U} \boldsymbol{f}^H_{d(u)} \boldsymbol{\Phi}_{d(u)} \boldsymbol{f}_{d(u)} \ , \quad (5)$$

where $\boldsymbol{\Phi}_{d(u)} = \mathrm{diag}\{\boldsymbol{\Phi}_{d(u),1}, \boldsymbol{\Phi}_{d(u),2}, \ldots, \boldsymbol{\Phi}_{d(u),M}\}$ is a block diagonal matrix whose blocks $\boldsymbol{\Phi}_{d(u),m}$ are Hermitian Toeplitz matrices with the first row

$$\left[\phi_{d(u),m}[0], \phi_{d(u),m}[-N], \ldots, \phi_{d(u),m}[-N(L_q - 1)]\right] \ ,$$

and $\phi_{d(u),m}[k] = p_{d(u),m}[k] * p^H_{d(u),m}[-k]$.

B. Filter Design for Multiuser Two-Way DTF Relaying

In this section we describe the design strategies for optimizing the uplink and downlink filter coefficients for the multiuser

two-way DTF relaying with self-interference cancelation at the nodes. For the uplink phase the equalizing filters are designed according to the MMSE criterion. In the downlink, the sum-MSE criterion is applied.

Using the description of the received signal in (3), and defining the uplink MSE as $\mathrm{MSE}^{\mathrm{UL}}_{s(u)} = \mathcal{E}\{|r^{\mathrm{UL}}_{s(u)} - a_{s(u)}[n-n_0]|^2\}$, the MSE in terms of the uplink filter coefficients is written as

$$\mathrm{MSE}^{\mathrm{UL}} = \Big\| \big[\boldsymbol{f}^{\mathrm{UL}^H}_{s(u)} \boldsymbol{W}^{\mathrm{UL}^H}_{s(1),s(u)}, \ldots, \boldsymbol{f}^{\mathrm{UL}^H}_{s(u)} \boldsymbol{W}^{\mathrm{UL}^H}_{s(u),s(u)} - \boldsymbol{e}_{n_0} , \ldots, \boldsymbol{f}^{\mathrm{UL}^H}_{s(u)} \boldsymbol{W}^{\mathrm{UL}^H}_{s(U),s(u)}, \sigma_R \boldsymbol{f}^{\mathrm{UL}^H}_{s(u)} \boldsymbol{P}^H_{s(1),s(u)} \big] \Big\|^2 . \tag{6}$$

Applying the Karush-Kuhn-Tucker (KKT) conditions, the solution for the uplink linear MMSE filter is obtained as

$$\boldsymbol{f}^{\mathrm{UL}}_{s(u)} = \Big(\sum_{\ell=1}^{U} \boldsymbol{W}^{\mathrm{UL}^H}_{s(\ell),s(u)} \boldsymbol{W}^{\mathrm{UL}}_{s(\ell),s(u)} + \sigma_z^2 \boldsymbol{P}^H_{s(u)} \boldsymbol{P}_{s(u)} \Big)^{-1} \boldsymbol{W}^H_{s(u),s(u)} \boldsymbol{e}_{n_0} . \tag{7}$$

In the downlink phase, if a PEF design without self-interference cancelation is considered, the design procedures from [4] can directly be applied to obtain the PEF coefficients. However, since the signal received at the destination contains the node's own transmitted message, it is reasonable to cancel the self-interference at the node and reduce the pre-equalization task. Due to the large delay spread of UWB channels, the received signal at the destination contains self-interference from more than one symbol of the destination's transmitted signal. Depending on the number of stored symbols, it is possible to cancel the effect of multiple transmitted symbols in the received signal. Note that self-interference cancelation requires feedback of the self-interference cancelation coefficients from the relay to the nodes. The coefficients have to be updated each time the PEFs or the channel change.

In the following we describe the PEF design for the downlink phase of DTF relaying, where different from the design developed in [4] self-interference cancelation is considered. As mentioned earlier the PEF coefficients are optimized based on a sum-MSE minimization design criterion. The MSE of the downlink transmission, at the destination node prior to detection is defined as

$$\mathrm{MSE}^{IC}_{d(u)} = \mathcal{E}\{|\alpha r_{d(u)}[n] - a_{s(u)}[n-2n_0] - \boldsymbol{\beta}^H_{d(u)} \bar{\boldsymbol{a}}_{d(u)}[n]|^2\} , \tag{8}$$

where $a_{s(u)}[n-2n_0]$ is the desired signal from source node $s(u)$, $\bar{\boldsymbol{a}}_{d(u)}[n]$ is an $L_t \times 1$ vector containing the stored transmitted symbols at the L_c indices selected for self-interference cancelation and zeros everywhere else, and the vector $\boldsymbol{\beta}_{d(u)} \in \mathbb{C}^{L_t \times 1}$ contains the self-interference cancelation coefficients at the L_c self-interference cancelation indices and zeros elsewhere. Note that this is a generalization to Figure 1, where only one-tap self-interference was shown as an example. The scaling factor α is related to the modified MSE definition from [35]. Therefore, setting the same scaling factor for all users, the MSE from Eq. (8) is

$$\mathrm{MSE}^{\mathrm{IC}}_{d(u)} = \| [\, \alpha \boldsymbol{f}^H_{d(1)} \boldsymbol{W}^H_{d(1),d(u)}, \ldots, \alpha \boldsymbol{f}^H_{d(u)} \boldsymbol{W}^H_{d(u),d(u)} - \boldsymbol{e}_{2n_0}, \alpha \boldsymbol{f}^H_{s(u)} \boldsymbol{W}^H_{s(u),d(u)} - \boldsymbol{\beta}^H_{d(u)}, \ldots, \alpha \boldsymbol{f}^H_{d(U)} \boldsymbol{W}^H_{d(U),d(u)}, \alpha \sigma_{d(u)} \,] \|^2 . \tag{9}$$

Using the MSE definition from Eq. (9), the sum-MSE minimization problem can be formulated as

$$\min_{\substack{\boldsymbol{f}_1,\ldots,\boldsymbol{f}_U,\alpha,\\ \boldsymbol{\beta}_1,\ldots,\boldsymbol{\beta}_U}} \quad \sum_{u=1}^{U} \mathrm{MSE}^{\mathrm{IC}}_{d(u)} , \tag{10a}$$

$$\text{s.t.} \quad \sum_{u=1}^{U} \boldsymbol{f}^H_{d(u)} \boldsymbol{\Phi}_{d(u)} \boldsymbol{f}_{d(u)} \leq P_{\max} . \tag{10b}$$

Setting $\boldsymbol{\beta}_{d(u)} = \alpha^H \boldsymbol{A}_{L_c} \boldsymbol{W}_{s(u),d(u)} \boldsymbol{f}_{s(u)}$, to cancel the self-interference from the L_c symbols, where $\boldsymbol{A}_{L_c} = \mathcal{E}\{\boldsymbol{a}_{d(u)}[n] \bar{\boldsymbol{a}}^T_{d(u)}[n]\}$, and applying the KKT conditions on the Lagrangian function for the above convex problem results in the following closed-form solution for the design parameters:

$$\alpha = \sqrt{\frac{1}{P_{\max}} \sum_{u=1}^{U} \boldsymbol{e}_{2n_0} \boldsymbol{W}_{d(u),d(u)} \boldsymbol{T}^H_{d(u)} \boldsymbol{\Phi}_{d(u)} \boldsymbol{T}_{d(u)} \boldsymbol{W}^H_{d(u),d(u)} \boldsymbol{e}_{2n_0}} , \tag{11}$$

and

$$\boldsymbol{f}_{d(u)} = \boldsymbol{T}_{d(u)} \boldsymbol{W}^H_{d(u),d(u)} \boldsymbol{e}_{2n_0} / \alpha , \tag{12}$$

where

$$\boldsymbol{T}_{d(u)} = \Big(\sum_{\ell=1}^{U} \boldsymbol{W}^H_{d(u),d(\ell)} \boldsymbol{W}_{d(u),d(\ell)} + \frac{\sum_{u=1}^{U} \sigma^2_{d(u)}}{P_{\max}} \boldsymbol{\Phi}_{d(u)} - \boldsymbol{W}^H_{d(u),s(u)} \boldsymbol{A}_{L_c} \boldsymbol{W}_{d(u),s(u)} \Big)^{-1} .$$

The number of operations associated with calculation of the uplink DTF relay filter $\boldsymbol{f}^{\mathrm{UL}}$ from Eq. (7) can be approximated as $O\big((ML_f)^3 + (ML_f)^2(UL_t + L_t + L_z + 1) + (ML_f)L_t\big)$. Similarly, for downlink DTF relay filter $\boldsymbol{f}$ from Eq. (12), the computational complexity is of the order of $O\big((ML_f)^3 + (ML_f)^2(UL_t + 2L_t + 2) + (ML_f)(L_t^2 + L_t)\big)$. In both cases the computational complexity is cubic in the filter length (ML_f). Hence reducing the filter length is highly desirable for practical implementation and to bound the computational complexity associated with calculation of the optimized filters. Note that in absence of post(/pre)-rake filters, filter lengths of the order of ML_h would be required to achieve a performance similar to that of our proposed design.

C. Filtering with User Specific Scaling Factors

The proposed design strategy in Section II-B is based on applying a single scaling factor α to all users. It was shown in [4] that assigning user specific scaling factors can improve the system performance and the interference cancelation characteristics of the system when users operate at different signal-to-noise ratio (SNR) levels. In this section the sum MSE filter design problem with self-interference cancelation from (10) is extended to allow for user specific scaling.

Including user specific scaling factors, the sum MSE optimization problem in Eq. (10) becomes non-convex. Therefore, we use the AO method from [13] to arrive at a solution.

Setting $\boldsymbol{\beta}_{d(u)} = \alpha_{d(u)}^H \boldsymbol{A}_{L_c} \boldsymbol{W}_{s(u),d(u)} \boldsymbol{f}_{s(u)}$, the Lagrangian function corresponding to the sum MSE minimization problem subject to a constraint on the total transmit power at the central relay is

$$\begin{aligned} L = U + \sum_{u=1}^{U} |\alpha_{d(u)}|^2 \sum_{\ell=1}^{U} \boldsymbol{f}_{d(\ell)}^H \boldsymbol{W}_{d(\ell),d(u)}^H \boldsymbol{W}_{d(\ell),d(u)} \boldsymbol{f}_{d(\ell)} - \\ \alpha_{d(u)} \boldsymbol{f}_{d(u)}^H \boldsymbol{W}_{d(u),d(u)}^H \boldsymbol{e}_{2n_0} - \alpha_{d(u)}^H \boldsymbol{e}_{2n_0}^T \boldsymbol{W}_{d(u),d(u)} \boldsymbol{f}_{d(u)} \\ + |\alpha_{d(u)}|^2 \Big(\sigma_{d(u)}^2 - \boldsymbol{f}_{s(u)}^H \boldsymbol{W}_{s(u),d(u)}^H \boldsymbol{A}_{L_c} \boldsymbol{W}_{s(u),d(u)} \boldsymbol{f}_{s(u)} \Big) \\ + \lambda \Big(\sum_{\ell=1}^{U} \boldsymbol{f}_{d(\ell)}^H \boldsymbol{\Phi}_{d(\ell)} \boldsymbol{f}_{d(\ell)} - P_{\max} \Big) , \end{aligned} \tag{13}$$

where λ is the Lagrange multiplier.

The AO method is an iterative procedure for optimizing a function jointly over a number of variables. The method is applicable to problems which are convex with respect to individual subsets of the variables and is based on dividing the parameter space into a number of non-overlapping subsets and alternating between restricted minimizations over each subset of variables [13]. For the sum MSE minimization problem, since the objective function is convex with respect to the individual subsets and is lower bounded by zero, the AO method always converges [9], [11], [12]. However, convergence to a globally optimum solution is not guaranteed. We derive closed-form solutions for updating the optimization parameters at each iteration until convergence to a local optimum.

In applying the alternating optimization method, the parameters from (13) are divided into three partitions, $\boldsymbol{\chi}_1 = [\alpha_{d(1)}, \ldots, \alpha_{d(U)}]$, $\boldsymbol{\chi}_2 = [\boldsymbol{f}_{d(1)}, \ldots, \boldsymbol{f}_{d(U)}]$ and $\chi_3 = \lambda$. Then in an iterative approach, for each of the partitions the restricted minimizer is computed while fixing all other parameters. The iterations stop if a maximum number of iterations is reached or if the change in the value of the parameters over all subsets and per iteration is smaller than a threshold ϵ. At each iteration t, the solutions are computed by applying the KKT conditions on the Lagrangian function in Eq. (13) as follows. The user specific scaling factors for each user are calculated and updated as per Eq. (14).

The downlink PEF coefficients are updated by setting

$$\boldsymbol{f}_{d(u)}^{(t+1)} = \boldsymbol{T}_{d(u)} \left(\boldsymbol{W}_{d(u),d(u)}^H \boldsymbol{e}_{2n_0} \right) \alpha_{d(u)}^{(t+1)} , \tag{15}$$

where

$$\begin{aligned} \boldsymbol{T}_{d(u)} = \Big| \alpha_{d(u)}^{(t+1)} \Big|^2 \Big(\sum_{\ell=1}^{U} \boldsymbol{W}_{d(u),d(\ell)}^H \boldsymbol{W}_{d(u),d(\ell)} \\ - \boldsymbol{W}_{d(u),s(u)}^H \boldsymbol{A}_{L_c} \boldsymbol{W}_{d(u),s(u)} + \lambda^{(t)} \boldsymbol{\Phi}_{d(u)} \Big)^{-1} . \end{aligned} \tag{16}$$

The Lagrangian coefficient λ is updated as

$$\lambda^{(t+1)} = \frac{\sum_{u=1}^{U} |\alpha_{d(u)}^{(t+1)}|^2 \sigma_{d(u)}}{P_{\max}} . \tag{17}$$

In the first iteration, the algorithm is initialized with the optimum solution from the design with identical α for all users in Eq. (11) and (12). After each iteration the difference in the vector containing all variables is calculated as $\boldsymbol{\Delta} = [\boldsymbol{\chi}_1^{(t+1)}, \boldsymbol{\chi}_2^{(t+1)}, \chi_3^{(t+1)}] - [\boldsymbol{\chi}_1^t, \boldsymbol{\chi}_2^t, \chi_3^t]$. The iterations stop if the maximum number of iterations is reached i.e., $t \geq N_{\text{iter}}$ or if $\|\boldsymbol{\Delta}\| \leq \epsilon$.

D. Widely Linear Filtering for Multiuser Two-Way DTF Relaying

Considering BPSK modulation in conjunction with UWB signalling in complex baseband representation, the real part of the received signal is a sufficient statistic for signal detection (see Eq. (1)). It was shown in [30] that PEF design, for DS-UWB with BPSK modulation, based on the real part of the received signal requires considerably lower transmit power. Hence, in this section we extend our relay filter design schemes to include this so-called widely linear (WL) filtering approach.

In the uplink phase, the WL uplink filter obtained according to the MMSE design is

$$\begin{aligned} \tilde{\boldsymbol{f}}_{s(u)}^{\text{UL}} = \Big(\sum_{\ell=1}^{U} (\tilde{\boldsymbol{W}}_{s(\ell),s(u)}^{\text{UL}})^T \tilde{\boldsymbol{W}}_{s(\ell),s(u)}^{\text{UL}} + \sigma_z^2/2 \tilde{\boldsymbol{P}}_{s(u)}^T \tilde{\boldsymbol{P}}_{s(u)} \Big)^{-1} \\ \tilde{\boldsymbol{W}}_{s(u),s(u)}^T \boldsymbol{e}_{n_0} , \end{aligned} \tag{18}$$

where

$$\tilde{\boldsymbol{W}}_{s(\ell),s(u)}^{\text{UL}} = [\Re\{\boldsymbol{W}_{s(\ell),s(u)}^{\text{UL}}\}, -\Im\{\boldsymbol{W}_{s(\ell),s(u)}^{\text{UL}}\}] ,$$

and

$$\tilde{\boldsymbol{P}}_{s(u)} = [\Re\{\boldsymbol{P}_{s(u)}\}, -\Im\{\boldsymbol{P}_{s(u)}\}] .$$

In the downlink phase, the MSE definition is modified as

$$\text{MSE}_{d(u)}^{IC} = \mathcal{E}\{|\alpha y_{d(u)}[n] - a_{s(u)}[n - 2n_0] - \boldsymbol{\beta}_{d(u)}^T \bar{\boldsymbol{a}}_{d(u)}[n]|^2\} , \tag{19}$$

where $y_{d(u)}[n]$ is the real part of the signal $r_{d(u)}[n]$.

The widely linear version of the downlink filters are obtained by replacing $\boldsymbol{f}_{d(u)}$ with $\tilde{\boldsymbol{f}}_{d(u)} = \Big[\Re\{\boldsymbol{f}_{d(u)}\}, \Im\{\boldsymbol{f}_{d(u)}\}\Big]$, replacing $\boldsymbol{W}_{d(\ell),d(u)}$ with $\tilde{\boldsymbol{W}}_{d(\ell),d(u)} = \Big[\Re\{\boldsymbol{W}_{d(\ell),d(u)}\}, \ -\Im\{\boldsymbol{W}_{d(\ell),d(u)}\}\Big]$, $\boldsymbol{\Phi}_{d(u)}$ with

$$\tilde{\boldsymbol{\Phi}}_{d(u)} = \begin{bmatrix} \Re\{\boldsymbol{\Phi}_{d(u)}\} & -\Im\{\boldsymbol{\Phi}_{d(u)}\} \\ \Im\{\boldsymbol{\Phi}_{d(u)}\} & \Re\{\boldsymbol{\Phi}_{d(u)}\} \end{bmatrix} ,$$

and $\sigma_{d(u)}^2$ by $\sigma_{d(u)}^2/2$ in equations (12) through (15).

E. Downlink BER Analysis

For the BPSK DS-UWB signaling, assuming residual noise and interference as Gaussian distributed, the bit error rate (BER) can be approximated in terms of the SINR at the detector prior to the sign operator as

$$\text{BER}_{d(u)} = Q\left(\sqrt{\text{SINR}_{d(u)}} \right) , \tag{20}$$

where $Q(.)$ denotes the Gaussian Q-function [36].

$$\alpha_{d(u)}^{(t+1)} = \frac{\Re\left\{ \boldsymbol{f}_{d(u)}^{(t)H} \boldsymbol{W}_{d(u),d(u)}^{H} \boldsymbol{e}_{2n_0} \right\}}{\sum_{\ell=1}^{U} \boldsymbol{f}_{d(\ell)}^{(t)H} \boldsymbol{W}_{d(\ell),d(u)}^{H} \boldsymbol{W}_{d(\ell),d(u)} \boldsymbol{f}_{d(\ell)}^{(t)} - \boldsymbol{f}_{s(u)}^{(t)H} \boldsymbol{W}_{s(u),d(u)}^{H} \boldsymbol{A}_{L_c} \boldsymbol{W}_{s(u),d(u)} \boldsymbol{f}_{s(u)}^{(t)} + \sigma_{d(u)}^2} \tag{14}$$

The SINR between the relay and the u^{th} pair's destination node $d(u)$ is derived as

$$\text{SINR}_{d(u)} = \frac{|\tilde{\boldsymbol{f}}_{d(u)}^{T} \tilde{\boldsymbol{W}}_{d(u),d(u)}^{T} \boldsymbol{e}_{n_0}|^2}{\sum_{\ell=1}^{U} \tilde{\boldsymbol{f}}_{d(\ell)}^{T} \tilde{\boldsymbol{W}}_{d(\ell),d(u)}^{T} \tilde{\boldsymbol{W}}_{d(\ell),d(u)} \tilde{\boldsymbol{f}}_{d(\ell)} - \rho_u + \frac{\sigma_{d(u)}^2}{2}} , \tag{21}$$

where $\rho_u = \|[\tilde{\boldsymbol{f}}_{d(u)}^{T} \tilde{\boldsymbol{W}}_{d(u),d(u)}^{T} \boldsymbol{e}_{n_0}, \tilde{\boldsymbol{f}}_{s(u)}^{T} \tilde{\boldsymbol{W}}_{s(u),d(u)}^{T} \boldsymbol{A}_{L_c}]\|^2$.

Note that the underlying Gaussian assumption is on the residual interference after pre/post-equalization. We have shown in [4] that for the downlink of a pre-equalized DS-UWB system the residual ISI and MUI at the receiving node is well approximated as Gaussian distributed. This result applies directly for the downlink phase of the DTF relaying setup considered here, and the same also applies for the residual interference after equalization in the uplink phase. This is also verified by numerical results, where simulation and analytical BER results show a close match. Furthermore, an end-to-end analysis of the BER for a pair of source and destination nodes requires an analytical representation of the error propagation in the uplink and the downlink phase. Since stream packetization and coding are not considered here, we do not perform any error propagation analysis.

III. Multiuser Two-Way Filter-and-Forward Relaying

In this section, filter design for multiuser two-way FF relaying is developed. Similar to the system model described in Section II-A, the signal processing at the source/destination nodes is relatively simple and inter-node communication is achieved through a central relay that is equipped with multiple antennas. The relay estimates the CSI between itself and the nodes, and handles the complexity associated with filtering. As it was mentioned in Section I, FF relaying can be considered as an extension of AF relaying over frequency selective channels [14]. The received signal at the relay is passed through a filter that is optimized to reduce the distortion caused by ISI and multiuser interference (MUI) in the multiple-access case [17]. We start by describing the relay structure and the signal representations and then proceed to developing the filter design procedures.

A. System Model

The general system model is fairly similar to the one introduced in Section II-A with the main difference being in the relay structure. In particular, the source and destination node structure is the same as the one considered in Section II-A and shown in Figure 1.

The block diagram of the central relay for half-duplex FF processing is shown in Figure 3. The received signal

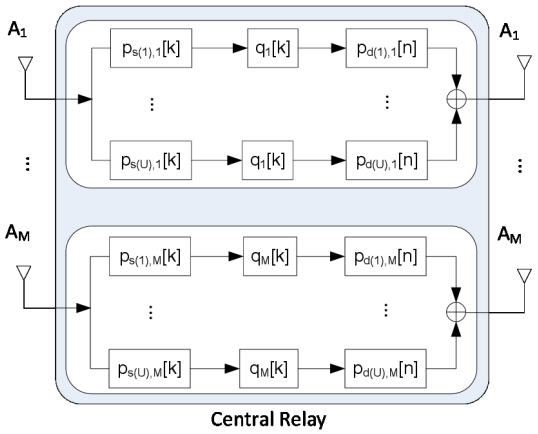

Fig. 3. Block diagram of the central relay with pre/post-rake filtering and multiuser two-way FF relaying.

at the relay's m^{th} antenna is rake combined based on the available channel coefficients of the link between source and relay through $\boldsymbol{p}_{s(u),m}$, and is then passed through an optimized filter $\boldsymbol{q}_m$ of length L_q, as shown in Figure 3. Prior to re-transmission, the signal is pre-rake combined with the estimated channel impulse response of the link between the relay and the destination node, $\boldsymbol{p}_{d(u),m}$. At each of the relay's antennas, the received signals from all transmitting users pass through the U pairs of source and destination pre/post rake filtering. Hence, we define $R_{sd,m}[k] = \sum_{\ell=1}^{U} \left(p_{s(\ell),m}[k] * p_{d(\ell),m}[k] \right)$. Then, the overall channel consisting of the transmit channel between source node $s(\ell)$ and the m^{th} antenna at the relay, the post/pre-rake combining filters, and transmit channel between the relay's m^{th} antenna and the destination node $d(u)$ is defined as $g_{s(\ell),m,d(u)}[k] = h_{s(\ell),m}[k] * R_{sd,m}[k] * h_{d(u),m}[k]$.

For the FF relaying scheme, the received signal at the destination node can be written as

$$r_{d(u)}[n] = \sum_{\ell=1}^{U} \boldsymbol{q}^H \boldsymbol{G}_{s(\ell),d(u)}^{H} \boldsymbol{a}_{s(\ell)}[n] + z_{d(u)}[n] + v_{d(u)}[n] , \tag{22}$$

where

- $\boldsymbol{q} = [\boldsymbol{q}_1^T, \ldots, \boldsymbol{q}_M^T]^T$ is the concatenated vector of the filter coefficients across all antennas,
- $\boldsymbol{q}_m = [q_m[0], \ldots, q_m[L_q - 1]]^H$ is the vector of filter coefficients at the m^{th} antenna,
- the matrix $\boldsymbol{G}_{s(\ell),d(u)}$ is the convolution-matrix containing the overall channel impulse response coefficients. It is defined as $\boldsymbol{G}_{s(\ell),d(u)} = [\boldsymbol{G}_{s(\ell),1,d(u)}, \ldots, \boldsymbol{G}_{s(\ell),M,d(u)}]$ and is a block matrix with block components $\boldsymbol{G}_{s(\ell),m,d(u)}$,
- $\boldsymbol{G}_{s(\ell),m,d(u)}$ is formed by downsampling the rows of Toeplitz matrix $\bar{\boldsymbol{G}}_{s(\ell),m,d(u)}$ by factor N,
- $\bar{\boldsymbol{G}}_{s(\ell),m,d(u)}$ is defined by first row

$[(g_{s(\ell),m,d(u)}[k_f])^*, \mathbf{0}_{L_q-1}]$, where the sampling phase k_f is set as $k_f = L_p + L_h - 2 - N\lfloor\frac{L_p+L_h-2}{N}\rfloor$, and first column $\Big[g_{s(\ell),m,d(u)}[k_f],\ g_{s(\ell),m,d(u)}[k_f+1], \ldots, g_{s(\ell),m,d(u)}[k_f+(2L_h+2L_p-4)], \mathbf{0}_{L_q-1}\Big]^H$,

- $\boldsymbol{a}_{s(\ell)}[n] = \big[a_{s(\ell)}[n], \ldots, a_{s(\ell)}[n-L_g+1]\big]^T$ is the $L_g \times 1$ vector of transmitted symbols affecting the received signal, where $L_g = \lceil\frac{2L_p+2L_h+L_q-4-k_f}{N}\rceil$,
- $z_{d(u)}[n] \sim \mathcal{N}(0, \sigma^2_{d(u)})$ is the additive white Gaussian noise (AWGN) at the destination node,
- $v_{d(u)}[n] = \sum_{m=1}^{M} v_{d(u),m}[n]$ is the colored noise that is added at the relay and is being processed and forwarded to the destination node. It is defined as $v_{d(u)}[n] = \boldsymbol{q}^H \boldsymbol{\Upsilon}^H_{d(u)} \boldsymbol{z}_R$, where $\boldsymbol{\Upsilon}_{d(u)} = \text{diag}\{\boldsymbol{\Upsilon}_{d(u),1}, \ldots, \boldsymbol{\Upsilon}_{d(u),M}\}$ is $ML_v \times ML_q$ and its block components $\boldsymbol{\Upsilon}_{d(u),m}$ are Toeplitz matrices with first row $[\Upsilon_{d(u),m}[0], \mathbf{0}_{L_q-1}]$ and first column $[\Upsilon_{d(u),m}[k_f], \Upsilon_{d(u),m}[k_f+1], \ldots, \Upsilon_{d(u),m}[k_f+(L_h+2L_p-3)], \mathbf{0}_{L_q-1}]$. $\Upsilon_{d(u),m} = R_{sd,m}[k] * h_{d(u),m}[k]$, $\boldsymbol{z}_{R,m}[n] = [z_{R,m}[n], z_{R,m}[n-1], \ldots, z_{R,m}[n-L_v+1]]$, and $z_{R,m}[k]$ is the AWGN added at the m^{th} antenna of the relay with variance $\sigma^2_{z_R}$. L_v is the length of the relay noise vector affecting the received colored noise at the destination node and is defined as $L_v = k_f + L_h + 2L_p - 3 + L_q$.

The average transmit power at the relay is the sum of the average power transmitted from the individual relay antennas. The transmit signal at the m^{th} antenna is $s_{R,m}[k] = (z_{R,m}[k] + \sum_{\ell=1}^{U} \tilde{a}_{s(\ell)}[k] * h_{\ell,m}[k]) * R_{sd,m}[k] * q_m[k]$, where $\tilde{a}_{s(\ell)}[k]$ represents the transmit symbol sequence upsampled by factor N. The average transmit power at the relay can be written as

$$P_R = \sum_{m=1}^{M} \mathcal{E}\{s_{R,m}[k] s^*_{R,m}[k]\} = \boldsymbol{q}^H \left(\sigma^2_{z_R} \boldsymbol{\Phi}_R + \sum_{\ell=1}^{U} \boldsymbol{\Phi}_{\Upsilon_{s(\ell)}}\right) \boldsymbol{q} \tag{23}$$

where the matrices $\boldsymbol{\Phi}_R$, and $\boldsymbol{\Phi}_{\Upsilon_{s(\ell)}}$ are block diagonal matrices with Hermitian Toeplitz block component matrices $\boldsymbol{\Phi}_{R,m}$ and $\boldsymbol{\Phi}_{\Upsilon_{s(\ell),m}}$, respectively. The first row of $\boldsymbol{\Phi}_{R,m}$ is defined as $[\phi_{R,m}[0], \phi_{R,m}[-1], \ldots, \phi_{R,m}[-L_q+1]]$, where $\phi_{R,m}[k] = R_{sd,m}[k] * R^*_{sd,m}[-k]$. The matrix $\boldsymbol{\Phi}_{\Upsilon_{s(\ell)}}$ is structured similarly to $\boldsymbol{\Phi}_R$ by replacing $\phi_{R,m}[k]$ with $\phi_{\Upsilon_{s(\ell)}}[k] = \Upsilon_{s(\ell),m}[k] * \Upsilon^*_{s(\ell),m}[-k]$.

B. Filter Design for Multiuser Two-Way FF Relaying

The FF strategy offers a simpler relay design and reduced delay compared to the DTF processing, since the messages from all nodes are transmitted simultaneously to the relay, filtered and retransmitted (there is no detection and remodulation prior to transmission from the relay to the destination node). In addition in the FF relaying scheme, all user messages are filtered by a single filter vector $\boldsymbol{q}$, hence the design has a smaller number of degrees of freedom compared to the DTF relaying scheme. Therefore, self-interference cancelation plays a critical role in improving the overall performance. Similar to the DTF relaying filter design in Section II-B, the sum-MSE is the criterion of choice for the filter design.

The MSE with self-interference cancelation at the destination node prior to detection is defined as

$$\text{MSE}^{\text{IC}}_{d(u)} = \mathcal{E}\left\{\left|\alpha r_{d(u)}[n] - a_{s(u)}[n-n_f] - \boldsymbol{\gamma}^H_{d(u)} \bar{\boldsymbol{a}}_{d(u)}[n]\right|^2\right\}, \tag{24}$$

where $\bar{\boldsymbol{a}}_{d(u)}[n]$ has the same definition as per Eq. (8), the vector $\boldsymbol{\gamma}_{d(u)} \in \mathbb{C}^{L_g \times 1}$ contains the self-interference cancelation coefficients at the L_c self-interference cancelation indices and zeros everywhere else, and delay n_f is set as $n_f = \lceil\lceil\frac{2L_h+2L_p+L_f-4-k_f}{N}\rceil/2\rceil$. Using the received signal representation from Eq. (22), the MSE is represented as

$$\begin{aligned}\text{MSE}^{\text{IC}}_{d(u)} = \Big\| \Big[&\alpha \boldsymbol{q}^H \boldsymbol{G}^H_{s(1),d(u)}, \ldots, \alpha \boldsymbol{q}^H \boldsymbol{G}^H_{s(u),d(u)} - \boldsymbol{e}_{n_f}, \\ &\ldots, \alpha \boldsymbol{q}^H \boldsymbol{G}^H_{d(u),d(u)} - \boldsymbol{\gamma}^H_{d(u)}, \ldots, \\ &\alpha \boldsymbol{q}^H \boldsymbol{G}^H_{s(U),d(u)}, \alpha\sigma_{d(u)}, \alpha\sigma_{z_R} \boldsymbol{q}^H \boldsymbol{\Upsilon}^H_{d(u)}\Big]\Big\|^2,\end{aligned} \tag{25}$$

where $\boldsymbol{e}_{n_f}$ is a vector with the n_f^{th} element set as 1 and zeros elsewhere. Assuming that factor α is identical for all users, and setting $\boldsymbol{\gamma}_{d(u)} = \alpha^H \boldsymbol{E}_{L_c} \boldsymbol{G}_{d(u),d(u)} \boldsymbol{q}$ with $\boldsymbol{E}_{L_c} = \mathcal{E}\{\boldsymbol{a}_{d(u)}[n] \bar{\boldsymbol{a}}^T_{d(u)}[n]\}$, then the sum-MSE design problem is written as

$$\min_{\boldsymbol{q},\alpha} \quad \sum_{u=1}^{U} \text{MSE}^{\text{IC,FF}}_{d(u)}, \tag{26a}$$

$$\text{s.t.} \quad \boldsymbol{q}^H \left(\sigma^2_{z_R} \boldsymbol{\Phi}_R + \sum_{u=1}^{U} \boldsymbol{\Phi}_{\Upsilon_{s(u)}}\right) \boldsymbol{q} \le P_{\max}. \tag{26b}$$

The above problem is in convex form, and applying KKT conditions, the closed-form solutions are found as

$$\alpha = \sqrt{\frac{\boldsymbol{e}^T_{n_f} \sum_{u=1}^{U} \boldsymbol{G}_{s(u),d(u)} \boldsymbol{T}^{\text{FF}^{\text{H}}} \boldsymbol{D} \boldsymbol{T}^{\text{FF}} \sum_{u=1}^{U} \boldsymbol{G}^H_{s(u),d(u)} \boldsymbol{e}_{n_f}}{P_{\max}}}, \tag{27}$$

where $\boldsymbol{D} = \sigma^2_{z_R} \boldsymbol{\Phi}_R + \sum_{u=1}^{U} \boldsymbol{\Phi}_{\Upsilon_{s(u)}}$,

$$\begin{aligned}\boldsymbol{T}^{\text{FF}} = \Big(&\sum_{i=1}^{U}\sum_{j=1}^{U} \boldsymbol{G}^H_{s(i),d(j)} \boldsymbol{G}_{s(i),d(j)} + \sigma^2_{z_R} \sum_{u=1}^{U} \boldsymbol{\Upsilon}^H_{d(u)} \boldsymbol{\Upsilon}_{d(u)} \\ &- \sum_{u=1}^{U} \boldsymbol{G}^H_{d(u),d(u)} \boldsymbol{E}_{L_c} \boldsymbol{G}_{d(u),d(u)} + \boldsymbol{D} \sum_{u=1}^{U} \frac{\sigma^2_{d(u)}}{P_{\max}}\Big)^{-1},\end{aligned}$$

and the downlink PEF is given as

$$\boldsymbol{q} = \boldsymbol{T}^{\text{FF}} \left(\sum_{u=1}^{U} \boldsymbol{G}^H_{s(u),d(u)}\right) \boldsymbol{e}_{n_f}/\alpha. \tag{28}$$

C. Iterative Design for User Specific Scaling Factors

In this section the design from Section III-B is extended to a more general case with user specific scaling for the individual source/destination nodes. Similar to Section II-C, an iterative design scheme is proposed based on minimizing the sum-MSE.

The MSE with self-interference cancelation and user specific scaling is defined as

$$\mathrm{MSE}_{d(u)}^{IC} = \mathcal{E}\{|\alpha_{d(u)} r_{d(u)}[n] - a_{s(u)}[n-n_f] - \boldsymbol{\gamma}_{d(u)}^H \bar{\boldsymbol{a}}_{d(u)}|^2\} \,. \tag{29}$$

Using the received signal representation from (22), the MSE is derived as per Eq. (30).

Next we use the AO approach to arrive at a solution for the sum MSE minimization problem subject to the maximum relay transmit power constraint. As mentioned earlier, for a non-convex optimization problem, the AO algorithm does not guarantee convergence to a global optimum point. The parameter space is divided as $\boldsymbol{\chi}_1 = [\alpha_{d(1)}, \ldots, \alpha_{d(U)}]$, $\boldsymbol{\chi}_2 = \boldsymbol{q}$ and $\chi_3 = \lambda$, where λ is a Lagrangian multiplier. Setting $\boldsymbol{\gamma}_{d(u)} = \alpha_{d(u)}^H \boldsymbol{E}_{L_c} \boldsymbol{G}_{d(u),d(u)} \boldsymbol{q}$, and using KKT conditions, the strict minimizers at each iteration index, t, are found as

$$\alpha_{d(u)}^{(t+1)} = \frac{\Re\{\boldsymbol{q}^{(t)H} \boldsymbol{G}_{s(u),d(u)}^H \boldsymbol{e}_{n_f}\}}{\boldsymbol{q}^{(t)H} \boldsymbol{\Gamma}_{d(u)} \boldsymbol{q}^{(t)} + \sigma_{d(u)}} \,, \tag{31}$$

where

$$\begin{aligned}\boldsymbol{\Gamma}_{d(u)} =& \sum_{\ell=1}^{U} \boldsymbol{G}_{s(\ell),d(u)}^H \boldsymbol{G}_{s(\ell),d(u)} - \boldsymbol{G}_{d(u),d(u)}^H \boldsymbol{E}_{L_c} \boldsymbol{G}_{d(u),d(u)} + \\ & \sigma_{z_R}^2 \boldsymbol{\Upsilon}_{d(u)}^H \boldsymbol{\Upsilon}_{d(u)} \,,\end{aligned} \tag{32}$$

$$\boldsymbol{q}^{(t+1)} = \boldsymbol{T}_{\alpha}{}^{(t+1)} \left(\sum_{u=1}^{U} \alpha_{d(u)}^{(t+1)} \boldsymbol{G}_{s(u),d(u)}^H \boldsymbol{e}_{n_f} \right) \,, \tag{33}$$

$$\boldsymbol{T}_{\alpha}^{(t+1)} = \Big(\sum_{u=1}^{U} |\alpha_{d(u)}^{(t+1)}|^2 \boldsymbol{\Gamma}_{d(u)} + \lambda^{(t)} \boldsymbol{D} \Big)^{-1} \,,$$

and

$$\lambda^{(t+1)} = \frac{\sum_{u=1}^{U} |\alpha_{d(u)}^{(t+1)}|^2 \sigma_{d(u)}^2}{P_{\max}} \,.$$

For the initial solution, the parameters from the optimal solution of the design with identical parameter α for all users from Eqs. (27) and (28) are used to solve Eq. (31), and (33) in the first iteration. After each iteration two conditions are checked as stopping criteria, (i) $\|\boldsymbol{\chi}^{(t+1)} - \boldsymbol{\chi}^t\| \leq \epsilon$, where $\boldsymbol{\chi}^t = [\boldsymbol{\chi}_1^t, \boldsymbol{\chi}_2^t, \chi_3^t]$, (ii) $t < N_{\mathrm{iter}}$, checking if the number of iteration has reached the maximum allowable number of iterations.

D. Widely Linear Filtering for Multiuser Two-Way FF Relaying

The widely linear counterparts of the filter design schemes introduced in Section III-B and Section III-C are obtained by incorporating the real part of the received signal in the MSE definitions of (24) and (29). The real part of the received signal is written as

$$y_{d(u)}[n] = \sum_{\ell=1}^{U} \tilde{\boldsymbol{q}}^T \tilde{\boldsymbol{G}}_{s(\ell),d(u)}^T \boldsymbol{a}_{s(\ell)}[n] + \tilde{z}_{d(u)}[n] + \tilde{v}_{d(u)}[n] \,, \tag{34}$$

where $\tilde{\boldsymbol{q}} = [\Re\{\boldsymbol{q}\}, \Im\{\boldsymbol{q}\}]$, $\tilde{\boldsymbol{G}}_{s(\ell),d(u)} = [\Re\{\boldsymbol{G}_{s(\ell),d(u)}\}, -\Im\{\boldsymbol{G}_{s(\ell),d(u)}\}]$, and the AWGN noise term $\tilde{z}_{d(u)}[n] = \mathcal{N}(0, \sigma_{d(u)}^2/2)$. The real part of the colored noise forwarded through the relay is written as $\tilde{v}_{d(u)}[n] = \tilde{\boldsymbol{q}}^T \tilde{\boldsymbol{\Upsilon}}_{d(u)}^T \tilde{\boldsymbol{z}}_R$, where $\tilde{\boldsymbol{z}}_R = [\Re\{\boldsymbol{z}_R\}, \Im\{\boldsymbol{z}_R\}]$ and

$$\tilde{\boldsymbol{\Upsilon}}_{d(u)} = \begin{bmatrix} \Re\{\boldsymbol{\Upsilon}_{d(u)}\} & -\Im\{\boldsymbol{\Upsilon}_{d(u)}\} \\ -\Im\{\boldsymbol{\Upsilon}_{d(u)}\} & -\Re\{\boldsymbol{\Upsilon}_{d(u)}\} \end{bmatrix} \,.$$

The matrices $\boldsymbol{\Phi}_R$ and $\boldsymbol{\Phi}_{\Upsilon_{s(u)}}$ are replaced with

$$\tilde{\boldsymbol{\Phi}}_R = \begin{bmatrix} \Re\{\boldsymbol{\Phi}_R\} & -\Im\{\boldsymbol{\Phi}_R\} \\ \Im\{\boldsymbol{\Phi}_R\} & \Re\{\boldsymbol{\Phi}_R\} \end{bmatrix} \,,$$

and

$$\tilde{\boldsymbol{\Phi}}_{\Upsilon_{s(u)}} = \begin{bmatrix} \Re\{\boldsymbol{\Phi}_{\Upsilon_{s(u)}}\} & -\Im\{\boldsymbol{\Phi}_{\Upsilon_{s(u)}}\} \\ \Im\{\boldsymbol{\Phi}_{\Upsilon_{s(u)}}\} & \Re\{\boldsymbol{\Phi}_{\Upsilon_{s(u)}}\} \end{bmatrix} \,.$$

E. BER Analysis

The BER for each of the source and destination pairs can again be approximated using the SINR for the corresponding link (assuming that the residual interference is Gaussian distributed). The SINR for the design with self-interference cancelation at the destination node $d(u)$, after the real operator is derived as per Eq. (35), where $\eta_{d(u)} = \frac{\sigma_{z_R}^2}{2} \tilde{\boldsymbol{q}}^T \tilde{\boldsymbol{\Upsilon}}_{d(u)}^T \tilde{\boldsymbol{\Upsilon}}_{d(u)} \tilde{\boldsymbol{q}} + \frac{\sigma_{d(u)}^2}{2}$.

Using the above definition for the SINR, the BER for the BPSK DS-UWB signaling can be evaluated as

$$\mathrm{BER}_{d(u)} = \mathrm{Q}\Big(\sqrt{\mathrm{SINR}_{d(u)}}\Big) \,. \tag{36}$$

IV. Numerical Results

In the following we describe and discuss a set of numerical results that demonstrate the performance of the two proposed relaying schemes. For the following numerical results, we consider the CM2 channel model for the residential non-line-of-sight environment, cf. [31], and the channel realizations are generated according to the procedure described in [37]. Note that the designs proposed in this paper are applicable to any UWB channel model. Our selection of CM2 from [31] as an example, is inspired by the potential application of our proposed system model for multimedia communications in residential non-line-of-sight environments [1]. The signaling specifications include a center frequency of 6 GHz and a pulse bandwidth of 0.5 GHz using root-raised cosine pulses $g_{\mathrm{Tx}}(t)$ and $g_{\mathrm{Rx}}(t)$ with roll-off 0.7. Unless otherwise specified, results are averaged over 500 channel realizations, and it is assumed that $\sigma_R^2 = \sigma_{d(1)}^2 = \ldots = \sigma_{d(U)}^2$, and that the uplink and downlink channel are of the same type.

$$\mathrm{MSE}_{d(u)}^{IC} = \Big\| \Big[\alpha_{d(u)} \boldsymbol{q}^H \boldsymbol{G}_{s(1),d(u)}^H, \ldots, \alpha_{d(u)} \boldsymbol{q}^H \boldsymbol{G}_{s(u),d(u)}^H - \boldsymbol{e}_{n_f}, \ldots, \alpha_{d(u)} \boldsymbol{q}^H \boldsymbol{G}_{d(u),d(u)}^H - \boldsymbol{\gamma}_{d(u)}^H, \ldots, \alpha_{d(u)} \boldsymbol{q}^H \boldsymbol{G}_{s(U),d(u)}^H, \alpha_{d(u)} \sigma_{d(u)}, \alpha_{d(u)} \sigma_{z_R} \boldsymbol{q}^H \boldsymbol{\Upsilon}_{d(u)}^H \Big] \Big\|^2 \tag{30}$$

$$\mathrm{SINR}_{d(u)} = \frac{|\tilde{\boldsymbol{q}}^T \tilde{\boldsymbol{G}}_{s(u),d(u)}^T \boldsymbol{e}_{n_f}|^2}{\sum_{\ell=1}^{U} \tilde{\boldsymbol{q}}^T \tilde{\boldsymbol{G}}_{s(\ell),d(u)}^T \tilde{\boldsymbol{G}}_{s(\ell),d(u)} \tilde{\boldsymbol{q}} - \|[\tilde{\boldsymbol{q}}^T \tilde{\boldsymbol{G}}_{s(u),d(u)}^T \boldsymbol{e}_{n_f}, \tilde{\boldsymbol{q}}^T \tilde{\boldsymbol{G}}_{d(u),d(u)}^T \boldsymbol{E}_{L_c}]\|^2 + \eta_{d(u)}} \tag{35}$$

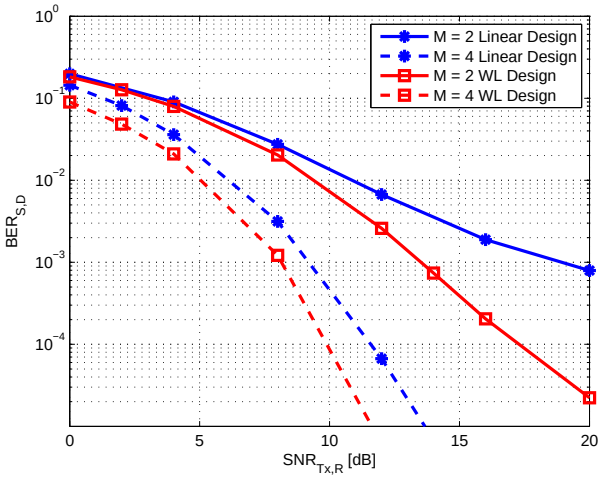

Fig. 4. BER between a pair of source and destination nodes versus relay transmit SNR, $\mathrm{SNR}_{\mathrm{Tx,R}} = P_{\max}/\sigma_{d(u)}^2$, shown for multiuser two-way DTF relaying with $U = 4$ users, $M = 2$ and $M = 4$ antennas at the relay and a PEF length of $L_f = 10$.

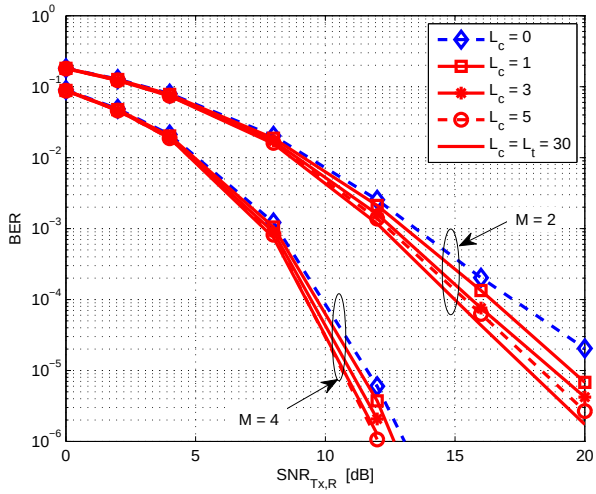

Fig. 5. BER between a pair of source and destination nodes versus relay transmit SNR, $\mathrm{SNR}_{\mathrm{Tx,R}} = P_{\max}/\sigma_{d(u)}^2$, shown for multiuser two-way DTF relaying with $U = 4$ users, $M = 2$ and $M = 4$ antennas at the relay and a PEF length of $L_f = 10$. WL design with identical scaling factor for all users. Comparison of the BER for self-interference cancelation lengths of $L_c = [1, 3, 5, 30]$.

A. Multiuser Two-Way DTF Relaying

In this section the simulated results for multiuser two-way DTF relaying are presented. In all results it is assumed that the filter lengths for uplink equalization and downlink pre-equalization are equal, i.e., $L_f^{\mathrm{UL}} = L_f$. We start by comparing the linear and widely linear design schemes. It was shown in [30] that the WL design scheme is preferred to its linear counter-part in terms of requiring lower minimum transmit power for meeting a pre-defined level of QoS. Here we compare the simulated BER between a pair of source and destination nodes, obtained using (10) with identical scaling factor for all users, for the linear and WL uplink and downlink filter designs.

In Figure 4, the simulated BER between a pair of source and destination nodes versus the relay transmit SNR, defined as $\mathrm{SNR}_{\mathrm{Tx,R}} = P_{\max}/\sigma_{d(u)}^2$, is shown for a network of $U = 4$ nodes communicating via the central relay (in bi-directional fashion). In the figure, the results for linear and WL designs are plotted for scenarios in which the central relay is equipped with $M = 2$ and $M = 4$ antennas, respectively. Considering a BER of 1×10^{-3} as a point of reference for the comparison, when $M = 2$, the WL design achieves the reference BER at a 5 dB lower transmit SNR than the linear design. Increasing the number of antennas at the relay to $M = 4$, the difference in transmit SNR is approximately 1.5 dB. The transmit SNR at the relay is a measure of the transmit power required for achieving the reference BER. Considering the superiority of the WL design approach, we select the WL design for generating the next sets of results in this section, that evaluate the performance of the DTF relaying scheme.

First, we study the effect of self-interference cancelation on the simulated BER. Figure 5 shows the BER between a pair of source and destination nodes versus the relay transmit SNR for $U = 4$ nodes and $M = 2$ and $M = 4$ antennas at the relay, respectively. Similar to the previous figure, the results are generated for the design problem from (10). The BER is simulated for the WL design without self-interference cancelation at the transceiver node ($L_c = 0$) and the WL design with self-interference cancelation for $L_c = 1, 3, 5, 30$, where $L_c = 30$ corresponds to full self-interference cancelation, i.e., canceling the effect of the entire sequence of symbols which affect the received signal. The effect of self-interference cancelation is more pronounced in the scenario with $M = 2$ antennas at the relay compared to the case with $M = 4$. For example at a BER of 1×10^{-4}, and for $M = 2$, the design with $L_c = 30$ requires 2.5 dB less transmit SNR compared to the design without self-interference cancelation. In the case of $M = 4$, the difference in the transmit SNR is on the order of 1 dB. Furthermore, it can be seen from the figure that most of the benefits of full self-interference cancelation can

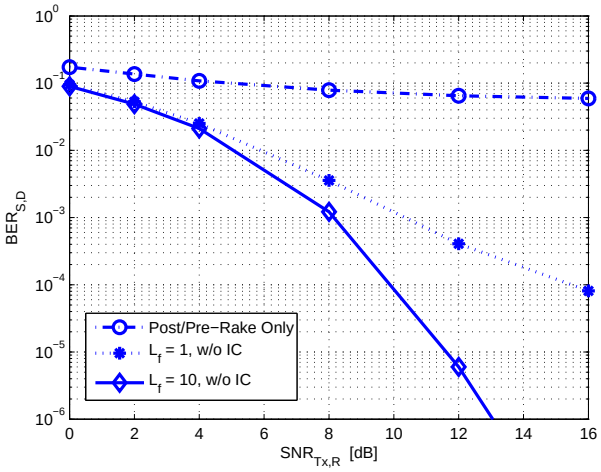

Fig. 6. BER between a pair of source and destination nodes versus relay transmit SNR, $\mathrm{SNR}_{\mathrm{Tx,R}} = P_{\max}/\sigma^2_{d(u)}$, shown for multiuser two-way DTF relaying with $U = 4$ users, and $M = 4$ antennas at the relay. WL design with identical scaling factor for all users. Comparison of the BER for post/pre-rake scheme without post/pre-equalization, post/pre-equalized DTF relaying with PEF length of $L_f = 1$ (single-tap beam-forming) and $L_f = 10$. w/o IC: without self-interference cancelation.

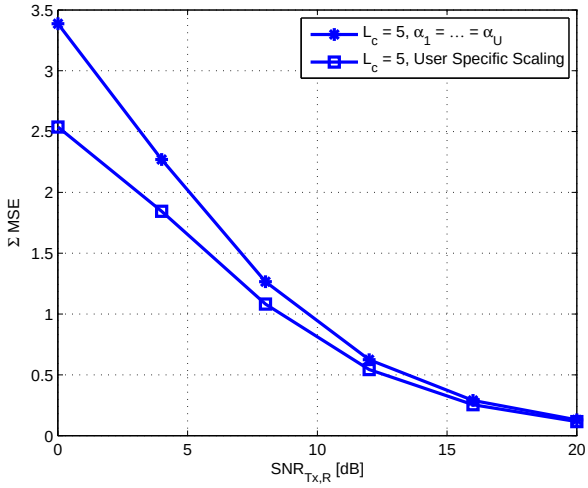

Fig. 7. Sum MSE versus relay transmit SNR, $\mathrm{SNR}_{\mathrm{Tx,R}} = P_{\max}/\sigma^2_{d(u)}$, shown for multiuser two-way DTF relaying with $U = 4$ users, $M = 4$ antennas at the relay and a PEF length of $L_f = 10$. WL design with self-interference cancelation and $L_c = 5$. Comparison between designs with identical receiver scaling factor for all users and the design with user specific scaling factors.

already be achieved by canceling the self-interference only from a small number of symbols. For the design scenarios in Figure 5, $L_c = 5$ achieves a performance that is close to that for full self-interference cancelation. Note that self-interference cancelation at the transceiver nodes requires i) feedback of self-interference cancelation coefficients from the destination node to the relay and ii) storing the transmitted symbols at the transceiver node. Hence reducing the number of self-interference cancelation symbols affects the feedback channel and the complexity of the operations (in terms of storage and recovery of symbols) at the transceiver nodes.

Figure 6 presents a comparison of our proposed DTF relaying scheme from Section II-B with two other DTF schemes namely, post/pre-rake without any post/pre-equalization, and the design with $L_f = 1$ which corresponds to single-tap beam-forming. We observe that rake combining in the uplink and pre-rake combining in the downlink are not sufficient to overcome the ISI and MUI. Furthermore, applying single tap beam-forming ($L_f = 1$), which is typically considered for relaying over flat fading MIMO channels, suffers from considerable residual interference, while our proposed design based on post-equalization in the uplink and pre-equalization in the downlink can fully eliminate the detrimental effects of ISI and MUI in UWB channels.

Next we proceed to discuss and present results related to the DTF relaying scheme with user specific scaling factors from Section II-C. In Figure 7, the downlink sum-MSE is plotted versus relay transmit SNR for $U = 4$ nodes, $M = 4$ antennas at the relay and a PEF length of $L_f = 10$. The noise variance at the relay and the transceiver nodes are set as follows: $\sigma^2_R = \sigma^2_{d(1)}$, and $\sigma^2_{d(u)}/\sigma^2_{d(1)} = 1, 2, 5, 10$ for user indices $u = 1, 2, 3, 4$ respectively. We observe from the figure that applying the iterative design for user specific scaling can improve the sum-MSE in the low-SNR regime.

For an in-depth study of the effect of user specific scaling, we consider a two user scenario. Figure 8 presents the sum-

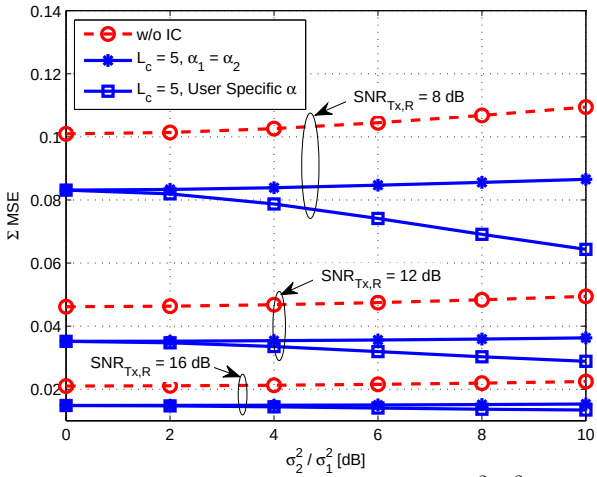

Fig. 8. Sum MSE versus user's noise level difference σ^2_2/σ^2_1 in dB, shown for multiuser two-way DTF relaying with WL design, $U = 2$ users, $M = 4$ antennas at the relay, and a PEF length of $L_f = 10$. Comparison between designs with and without self-interference cancelation (w/o IC), and identical receiver scaling factor for all users and the design with user specific scaling factors with self-interference cancelation.

MSE as a function of the difference in node's noise levels for several transmit SNR values set as $\mathrm{SNR}_{\mathrm{Tx,R}} = 8, 12, 16$ dB. As it can be seen from the figure, the efficacy of the iterative design for user specific scaling varies with the transmit SNR and also the difference in the receiving node noise levels. If users operate at similar noise levels, both solutions lead to the same performance (note that the iterative solution is initialized using the convex solution from (10)), hence the convex solution is more efficient in terms of the computation load at the relay. The relay can switch to the iterative approach to improve the overall performance if the channel and system conditions change.

B. Multiuser Two-Way FF Relaying

In this section we present and discuss the results related to the multiuser two-way FF relaying scheme. Similar to

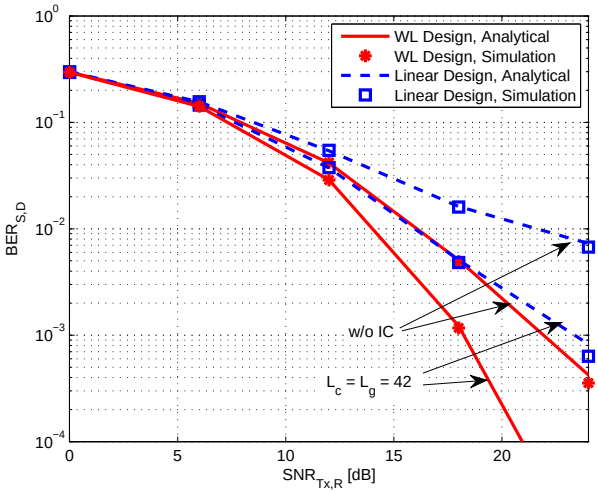

Fig. 9. BER between a pair of source and destination nodes versus relay transmit SNR, $\mathrm{SNR}_{\mathrm{Tx,R}} = P_{\max}/\sigma^2_{d(u)}$, shown for multiuser two-way FF relaying with $U = 4$ users, $M = 4$ antennas at the relay and a filter length of $L_q = 20$. Comparison between linear and widely linear designs, with and without self-interference cancelation and identical scaling factor for all users.

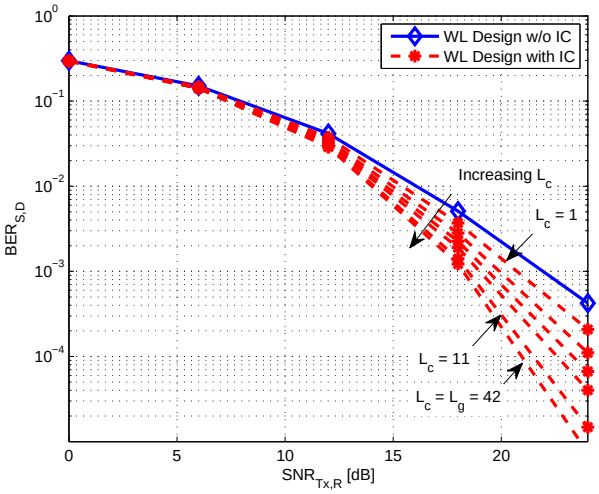

Fig. 10. Analytical BER between a pair of source and destination nodes versus the relay transmit SNR, $\mathrm{SNR}_{\mathrm{Tx,R}} = P_{\max}/\sigma^2_{d(u)}$, shown for multiuser two-way FF relaying with $U = 4$ users, $M = 4$ antennas at the relay and a filter length of $L_q = 20$. WL design with identical scaling factor for all users. Comparison of the BER for self-interference cancelation lengths of $L_c = [1, 3, 5, 7, 11, 42]$.

Section IV-A, we start by comparing the linear and WL design approaches and then proceed to a more detailed system performance evaluation.

In Figure 9, the pairwise BER for linear and WL schemes is shown for two design scenarios, with and without self-interference cancelation. For the simulations $U = 4$ transceiver nodes, $M = 4$ antennas at the relay and an equalization filter length of $L_q = 20$ is considered. As per the relay block diagram in Figure 3, the received signal at the relay is processed with a combination of post-and-pre-rake filters in addition to the equalizing filter prior to re-transmission. In case of self-interference cancelation, L_c is set to $L_c = 42$ which corresponds to full self-interference cancelation. The close match of the simulated results with that of the analytical evaluation from (36) confirms the validity of the derivations in Section III-E. It is observed that applying the WL design without self-interference cancelation achieves a BER that is comparable to the BER for the linear design with full self-interference cancelation. Considering that the gains achieved by the WL design come without any transmission overhead, unlike the self-interference cancelation scheme that requires feedback of information and storing the transmitted symbols, applying the WL design is clearly advantageous.

The effect of self-interference cancelation on the WL design of filters for multiuser two-way FF relaying with $U = 4$ users and relaying via $M = 4$ antennas at the relay, for the design with identical receiver scaling is depicted in Figure 10 (analytical results based on Eq. (36)). Self-interference cancelation lengths of $L_c = 1, 3, 5, 7, 11, 42$ are considered for comparison. It can be seen from the figure that increasing the number of self-interference cancelation symbols, improves the BER significantly. As an example, applying $L_c = 42$, a BER of 1×10^{-3} is achieved at 5 dB lower relay transmit SNR compared to the case with $L_c = 0$, which is quite significant compared to the gains achieved from self-interference cancelation in the DTF scheme (referring to Figure 5). It is also observed that $L_c = 11$ results in a performance comparable

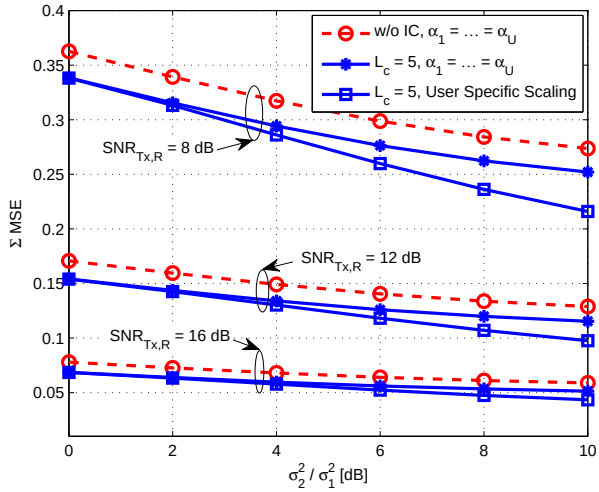

Fig. 11. Sum MSE versus user's noise level difference σ_2^2/σ_1^2 in dB, for FF relaying with $U = 2$ users, $M = 4$ antennas at the relay and equalization filter length $L_q = 20$. Comparison between WL designs with and without self-interference cancelation and identical receiver scaling factor for all users and the WL design with user specific scaling factors, with self-interference cancelation.

to $L_c = L_g = 42$. Such numerical evaluations based on Eq. (36), can be used at the relay to set the value of L_c.

Next, we proceed to evaluate the effect of the iterative design with user specific scaling on the overall performance. In Figure 11, the sum-MSE is plotted versus the noise level difference for a FF relaying network consisting of $U = 2$ nodes, $M = 4$ antennas at the relay, and the equalizing filter length set as $L_q = 20$. The sum-MSE is plotted for three transmit SNR levels of $\mathrm{SNR}_{\mathrm{Tx,R}} = 8, 12, 16$ dB. It is observed that at higher transmit SNR levels, the iterative design with user specific scaling achieves a sum-MSE that is comparable to that achieved by the non-iterative convex design with identical receiver scaling for all users. The effect of user specific scaling factors is more pronounced at lower transmit SNR levels and when the two users operate at different receive SNR levels.

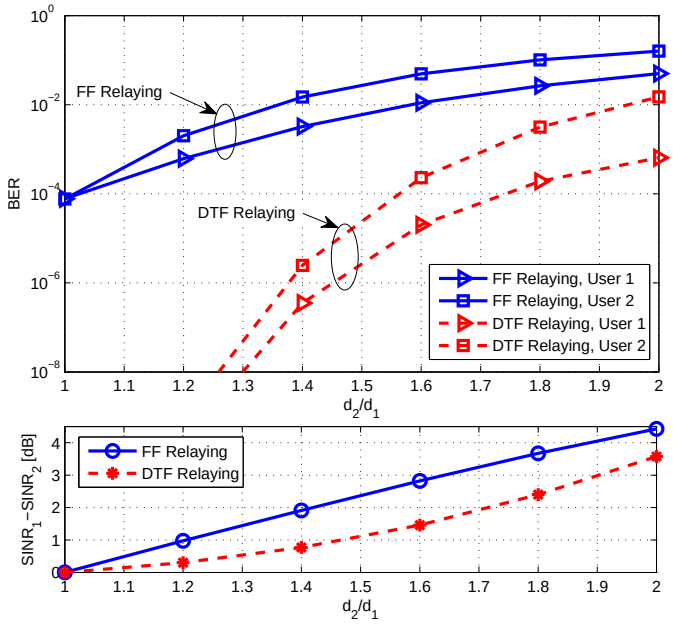

Fig. 12. The BER and SINR difference versus the ratio of the two users' distances from the relay d_2/d_1, for DTF and FF relaying with WL design, $U = 2$ users, $M = 4$ antennas at the relay, $\mathrm{SNR}_{\mathrm{Tx,R}} = 12\mathrm{dB}$ and equalization filter length of $L_q = 10$ for the DTF and $L_q = 20$ for the FF relaying scheme. Self-interference cancelation of length $L_c = 5$ and identical receiver scaling factor for all users are considered for both design schemes.

Note that the difference in noise levels translates to difference in received SNR. Therefore, the convex design scheme with identical scaling factor for all users can be used as the default FF relaying design procedure. Once the optimal solution of the design problem in (26) is obtained, the received SINR can be evaluated analytically using (35). Combining the information about the relay transmit SNR and the destination node SINR levels, the relay can make a decision about whether or not switching to the iterative design is useful.

For the final set of results, we study the effect of distance dependent path loss on the performance of the FF and DTF relaying schemes. For the purpose of comparison we consider two-way relaying between a pair of nodes, i.e. $U = 2$, with asymmetric distances from the relay. The distances between the relay and the two users are denoted as d_1 and d_2. The path loss exponent is set as 4.58, as per the recommendation from [31] for the CM2 model. The performance of the system is examined at discrete locations along a circle centered around the first user, the ratio d_2/d_1 is set to $d_2/d_1 = 1, 1.2, 1.4, 1.6, 1.8, 2$. Figure 12, shows the BER and the SINR difference, $\mathrm{SINR}_1 - \mathrm{SINR}_2$ in dB, versus the distance ratio of the two users, d_2/d_1 at a relay transmit SNR of 12 dB. For both relaying schemes, WL design with self-interference cancellation length of $L_c = 5$ are considered. As it can be seen from the figure, when both users are at the same distance from the relay, the users operate at same SINR levels and hence achieve similar BERs. Increasing the relay's distance from the second user, although the relay's distance from the first user is constant, both users experience a loss in BER which corresponds to approximately 4.5 dB SINR difference between the two users for the FF relaying and 3.5 dB downlink SINR difference in the DTF relaying scheme, when d_2 is set to be twice the value of d_1.

V. Concluding Remarks

In this paper we have developed two novel multiuser two-way relaying techniques, for a network of low-complexity DS-UWB nodes communicating via a more powerful central relay. The designs are based on DTF and FF processing at the relay. Our design schemes are novel in that we consider relaying over frequency-selective fading channels and the use of post/pre-rake combining. Considering BPSK DS-UWB signaling, WL counter-parts of the proposed filter design schemes were devised and the superiority of the WL designs for both relay schemes was demonstrated via numerical performance evaluation.

For both relaying schemes we formulated convex optimization problems with closed-form solution and also a more general formulation with an iterative design approach using alternating optimization. Based on numerical evaluations, for both schemes the benefits of the iterative design are notable when users operate at different SNR levels. Using our BER analysis, we suggest adopting the convex designs with identical receiver scaling for all users as the default design procedure for both schemes and switching to the iterative design when signaling conditions change.

The example results on self-interference cancelation, for channels randomly drawn from the CM2 UWB channel model, reveal that canceling the self-interference resulting from a small number of transmitted symbols, e.g. setting $L_c = 5$ for DTF relaying and $L_c = 11$ for FF relaying, is sufficient to achieve a performance close to the full self-interference cancelation while reducing the complexity at the receiving nodes. We note that the reported numbers vary for different channel models. Reducing the number of self-interference cancelation symbols is desired since it affects the traffic on the feedback channel and the processing at the destination nodes. Incorporating the uncertainty of the channel estimation into a robust design of the proposed relaying strategies is an interesting extension that will be considered as part of our future work.

References

[1] W. Jones, "No Strings Attached," *IEEE Spectr.*, vol. 43, pp. 16–18, Apr. 2006.

[2] G. Khuandaga, A. Iqbal, and K.-S. Kwak, "Performance Analysis of Modulation Schemes in Intra Vehicle Communications (IVC) Channel," in *International Conference on Advanced Communication Technology (ICACT)*, 2011, pp. 725–729.

[3] N. Sasaki, K. Kimoto, W. Moriyama, and T. Kikkawa, "A Single-Chip Ultra-Wideband Receiver With Silicon Integrated Antennas for Inter-Chip Wireless Interconnection," *IEEE J. Solid-State Circuits*, vol. 44, no. 2, pp. 382–393, 2009.

[4] Z. Ahmadian, M. B. Shenouda, and L. Lampe, "Design of Pre-Rake DS-UWB Downlink with Pre-Equalization," *IEEE Trans. Commun.*, vol. 60, no. 2, pp. 400–410, Feb. 2012.

[5] T. Kaiser and F. Zheng, *Ultra Wideband Systems with MIMO*. John Wiley & Sons, Inc., 2010.

[6] B. Rankov and A. Wittneben, "Spectral Efficient Protocols for Half-Duplex Fading Relay Channels," *IEEE J. Select. Areas Commun.*, vol. 25, no. 2, pp. 379–389, 2007.

[7] D. Gunduz, A. Yener, A. Goldsmith, and H. Poor, "The Multi-Way Relay Channel," in *Proc. IEEE International Symposium on Information Theory (ISIT)*, Jun. 2009, pp. 339 – 343.

[8] J. Joung and A. Sayed, "Multiuser Two-Way Amplify-and-Forward Relay Processing and Power Control Methods for Beamforming Systems," *IEEE Trans. Signal Processing*, vol. 58, no. 3, pp. 1833–1846, 2010.

[9] P. Ubaidulla and A. Chockalingam, "Relay Precoder Optimization in MIMO-Relay Networks With Imperfect CSI," *IEEE Trans. Signal Processing*, vol. 59, no. 11, pp. 5473–5484, 2011.

[10] G. Amarasuriya, C. Tellambura, and M. Ardakani, "Multi-Way MIMO Amplify-and-Forward Relay Networks with Zero-Forcing," in *Proc. IEEE Global Communications Conference (GLOBECOM)*, 2012, pp. 4689–4694.

[11] H. Mu and J. Tugnait, "MSE-Based Source and Relay Precoder Design for Cognitive Multiuser Multi-Way Relay Systems," *IEEE Trans. Signal Processing*, vol. 61, no. 7, pp. 1770–1785, 2013.

[12] M. Zhang, H. Yi, H. Yu, H. Luo, and W. Chen, "Joint Optimization in Bidirectional Multi-User Multi-Relay MIMO Systems: Non-Robust and Robust Cases," *IEEE Trans. Veh. Technol.*, 2013. [Online]. Available: http://dx.doi.org/10.1109/TVT.2013.2255898.

[13] J. Bezdek and R. Hathaway, "Some Notes on Alternating Optimization," in *Advances in Soft Computing AFSS 2002*, ser. Lecture Notes in Computer Science, N. Pal and M. Sugeno, Eds. Springer Berlin / Heidelberg, 2002, vol. 2275, pp. 187–195.

[14] H. Chen, A. Gershman, and S. Shahbazpanahi, "Filter-and-Forward Distributed Beamforming in Relay Networks With Frequency Selective Fading," *IEEE Trans. Signal Processing*, vol. 58, no. 3, pp. 1251–1262, Mar. 2010.

[15] Y. wen Liang, A. Ikhlef, W. Gerstacker, and R. Schober, "Cooperative Filter-and-Forward Beamforming for Frequency-Selective Channels with Equalization," *IEEE Trans. Wireless Commun.*, vol. 10, no. 1, pp. 228–239, Jan. 2011.

[16] ——, "Two-Way Filter-and-Forward Beamforming for Frequency-Selective Channels," *IEEE Trans. Wireless Commun.*, vol. 10, no. 12, pp. 4172–4183, Dec. 2011.

[17] H. Chen, S. Shahbazpanahi, and A. Gershman, "Filter-and-Forward Distributed Beamforming for Two-Way Relay Networks With Frequency Selective Channels," *IEEE Trans. Signal Processing*, vol. 60, no. 4, pp. 1927–1941, Apr. 2012.

[18] A. Schad, H. Chen, A. Gershman, and S. Shahbazpanahi, "Filter-and-Forward Multiple Peer-to-Peer Beamforming in Relay Networks with Frequency Selective Channels," in *IEEE International Conference on Acoustics Speech and Signal Processing (ICASSP)*, March 2010, pp. 3246–3249.

[19] C. Cho, H. Zhang, and M. Nakagawa, "A Short Delay Relay Scheme Using Shared Frequency Repeater for UWB Impulse Radio," *IEICE Transactions*, vol. 90-A, no. 7, pp. 1444–1451, 2007.

[20] C. Abou-Rjeily and A.-R. Marmar, "Novel high-rate transmit diversity schemes for MIMO IR-UWB and delay-tolerant Decode-and-Forward IR-UWB transmissions," in *Proc. IEEE International Conference on Ultra-Wideband (ICUWB)*, 2009, pp. 306–311.

[21] Z. Zeinalpour-Yazdi, M. Nasiri-Kenari, and B. Aazhang, "Performance of UWB Linked Relay Network with Time-Reversed Transmission in the Presence of Channel Estimation Error," *IEEE Trans. Wireless Commun.*, vol. 11, no. 8, pp. 2958–2969, 2012.

[22] X. Dong and X. Dong, "Bi-Directional Cooperative Relays for Transmitted Reference Pulse Cluster UWB Systems," in *Proc. IEEE Global Telecommunications Conference (GLOBECOM)*, 2010, pp. 1–5.

[23] Z. Wang, T. Lv, H. Gao, and Y. Li, "A Novel Two-Way Relay UWB Network with Joint Non-Coherent Detection in Multipath," in *Proc. IEEE Vehicular Technology Conference (VTC)*, 2011, pp. 1–5.

[24] M. Hamdi, J. Mietzner, and R. Schober, "Double-Differential Encoding for Dual-Hop Amplify-and-Forward Relaying in IR-UWB Systems," in *Proc. IEEE Vehicular Technology Conference (VTC)*, 2010, pp. 1–5.

[25] ——, "Multiple-Differential Encoding for Multi-Hop Amplify-and-Forward IR-UWB Systems," *IEEE Trans. Wireless Commun.*, vol. 10, no. 8, pp. 2577–2591, 2011.

[26] K. Maichalernnukul, T. Kaiser, and F. Zheng, "Performance Investigation of a UWB Relay System using Multiple Relays with Multiple Antennas in IEEE 802.15.3a Channel," in *Proc. IEEE Vehicular Technology Conference (VTC)*, 2009, pp. 1–6.

[27] K. Maichalernnukul, F. Zheng, and T. Kaiser, "Design and Performance of Dual-Hop MIMO UWB Transmissions," *IEEE Trans. Veh. Technol.*, vol. 59, no. 6, pp. 2906–2920, 2010.

[28] Z. Ahmadian and L. Lampe, "Robust Design of Widely Linear Pre-Equalization Filters for Pre-Rake UWB Systems," *IEEE Trans. Commun.*, vol. 61, no. 10, pp. 4206–4217, Oct. 2013.

[29] M. Joham, R. Irmer, S. Berger, G. Fettweis, and W. Utschick, "Linear Precoding Approaches for the TDD DS-CDMA Downlink," in *Proc. International Symposium on Wireless Personal Multimedia Commun. (WPMC)*, vol. 3, Oct. 2003, pp. 323–327.

[30] Z. Ahmadian and L. Lampe, "Widely Linear Design of Pre-Equalization Filters for Multiuser Pre-Rake UWB Systems," in *Proc. IEEE International Conference on Ultra-Wideband (ICUWB)*, Sep. 2011, pp. 278–282.

[31] A. F. Molisch, D. Cassioli, C.-C. Chong, S. Emami, A. Fort, B. Kannan, J. Karedal, J. Kunisch, H. G. Schantz, K. Siwiak, and M. Z. Win, "A Comprehensive Standardized Model for Ultrawideband Propagation Channels," *IEEE Trans. Antennas Propagat.*, vol. 54, no. 11, pp. 3151–3166, Nov. 2006.

[32] T. Strohmer, M. Emami, J. Hansen, G. Papanicolaou, and A. Paulraj, "Application of Time-Reversal with MMSE Equalizer to UWB Communications," in *Proc. IEEE Global Telecommun. Conf. (GLOBECOM)*, vol. 5, Dec. 2004, pp. 3123–3127.

[33] M. Emami, M. Vu, J. Hansen, A. Paulraj, and G. Papanicolaou, "Matched Filtering with Rate Back-off for Low-Complexity Communications in Very Large Delays Spread Channels," in *Proc. 38th Asilomar Conf. Signals, Systems, and Computers (ASILOMAR)*, Nov. 2004, pp. 218–222.

[34] E. Torabi, J. Mietzner, and R. Schober, "Pre-Equalization for MISO DS-UWB Systems with Pre-Rake Combining," *IEEE Trans. Wireless Commun.*, vol. 8, no. 3, pp. 1295–1307, Mar. 2009.

[35] M. Joham, K. Kusume, M. Gzara, W. Utschick, and J. Nossek, "Transmit Wiener Filter for the Downlink of TDDDS-CDMA Systems," in *IEEE International Symposium on Spread Spectrum Techniques and Applications*, vol. 1, Sep. 2002, pp. 9–13.

[36] J. Proakis, *Digital Communications*, 4th ed. McGraw Hill, 2000.

[37] A. F. Molisch et al., "IEEE 802.15.4a Channel Model - Final Report," Tech. Rep., 2005, document 802.1504-0662-01-004a.

Zahra Ahmadian (S'04, M'14) received her B.Sc. in Electrical Engineering from Ajman University of Science and Technology (AUST), UAE in 2005 and her M.A.Sc. and Ph.D. in Electrical and Computer Engineering from the University of British Columbia (UBC), Canada in 2007 and 2013 respectively. She was the recipient of the NSERC PGSM scholarship in 2006, NSERC CGSD scholarship in 2009, and was selected as the Google Anita Borg scholar in 2011. She is currently with Telus Mobility in Canada and also serves as the Chair of the Women in Engineering Committee on board IEEE Canada. Her research interests are ultra-wideband technology, multiuser interference mitigation, network security, optimization and statistical signal processing.

Lutz Lampe (M'02, SM'08) received his Diplom (Univ.) and Ph.D. degrees in electrical engineering from the University of Erlangen, Germany, in 1998 and 2002, respectively. Since 2003 he has been with the Department of Electrical and Computer Engineering at the University of British Columbia, where he is a full professor. His research interests are broadly in theory and application of wireless and power line communications.

He is (co-)recipient of a number of Best Paper Awards, including awards at the 2006 IEEE International Conference on Ultra-Wideband (ICUWB), 2010 IEEE International Communications Conference (ICC) and 2011 IEEE International Conference on Power Line Communications (ISPLC). He was awarded the Friedrich Wilhelm Bessel Research Award by the Alexander von Humboldt Foundation in 2009. He is currently an Associate Editor for the IEEE Wireless Communications Letters and the IEEE Communications Surveys and Tutorials, and has served as Associate and Guest Editor for several IEEE Transactions and journals. He was the General Chair of ISPLC 05 and ICUWB 09, and he is a General Co-Chair of the 2013 IEEE International Conference on Smart Grid Communications (SmartGridComm). He is the Chair of the IEEE Communications Society Technical Committee on Power Line Communication.

Jan Mietzner (S'02, M'08, SM'14) was born in Rendsburg, Germany in 1975. He studied electrical engineering at the Christian-Albrechts University (CAU) of Kiel, Germany, with focus on digital communications. During his studies, he spent 6 months in 2000 with the Global Wireless Systems Research Group, Lucent Technologies, Bell Labs UK, in Swindon, England. From 2001 to 2006, he was working toward his Ph.D. degree at the Information and Coding Theory Lab, CAU Kiel, and received his Ph.D. degree in December 2006. He received an award from the Friends of the Faculty of Engineering for the best dissertation in 2006. From January 2007 to December 2008, he was with the Department of Electrical and Computer Engineering at the University of British Columbia, in Vancouver, Canada, as a post-doctoral research fellow sponsored by the German Academic Exchange Service (DAAD). In March 2009, he joined Airbus in Ulm, Germany. His research interests concern physical layer aspects of future wireless communication systems, especially multiple-antenna techniques, ultrawideband and cognitive radio systems, relaying, and cooperative diversity techniques, as well as theoretical aspects of jamming and radar systems. He has published 40 papers in international journals and conference proceedings and is a co-recipient of the 2010 Best Paper Award from the German Information Technology Society (VDE/ITG). Dr. Mietzner has also served as a TPC member for various international conferences such as IEEE Globecom and ICC, and as Track Co-Chair for VTC-Fall 2014.